

Table II. Genes identified by MCA-RDA with CRCs positive or negative for *MLH1* methylation

Gene	GenBank accession no.	No. of MCA-RDA clones	Position of MCA-RDA clones	COBRA data
<i>Homo sapiens</i> , solute carrier family 38, member 3	BC042875	11	Promoter	N.D.
<i>Homo sapiens</i> hypothetical protein MGC29643 <sup>a</sup>	AK075487	10	Promoter	compatible
Human progesterone receptor	M15716	6	Exon 1	N.D.
<i>Homo sapiens</i> alpha-1 type XV collagen	L25286	6	Promoter	N.D.
<i>Homo sapiens</i> K-CI co-transporter KCC4	AF105365	5	Promoter	N.D.
<i>Homo sapiens</i> CGI-150 protein	AF151908	5	3' region	N.D.
<i>Homo sapiens</i> cDNA FLJ37615	AK094934	4	3' region	N.D.
Human mRNA and promoter DNA for progesterone receptor	X51730	3	Promoter	N.D.
Human arachidonate 12-lipoxygenase mRNA	M62982	3	Promoter	not compatible
<i>Homo sapiens</i> clone IMAGE:5173621	BC031660	3	Promoter	N.D.
<i>Homo sapiens</i> Ras and Rab interactor 1	BC014417	3	3' region	N.D.
<i>Homo sapiens</i> papilin (PAPLN) <sup>a</sup>	BC042057	3	Promoter	compatible
<i>Homo sapiens</i> F-box and leucine-rich repeat protein 7 (FBXL7) <sup>a</sup>	AB020647	3	Promoter	compatible
<i>Homo sapiens</i> fibronectin type 3 and ankyrin repeat domains 1	BC024189	3	Promoter	not compatible
BX444427 <i>Homo sapiens</i> ADULT BRAIN <i>Homo sapiens</i> cDNA clone	BX444427	3	Promoter	N.D.
UI-H-BW0-aju-d-09-0-UI.s1 NCL_CGAP_Sub6 <i>Homo sapiens</i> cDNA clone	AW297872	2	N.D.	N.D.
Human dystrobrevin-delta	U26742	2	Near 5' end	N.D.
<i>Homo sapiens</i> , clone IMAGE:5728979	BC035731	2	Promoter	compatible
<i>Homo sapiens</i> ras interactor (RIN1)	L36463	2	Promoter	N.D.
<i>Homo sapiens</i> partial mRNA for doublesex-mab-3 (DM) domain	AJ301580	2	Promoter	not compatible
<i>Homo sapiens</i> mRNA; cDNA DKFZp586D0619	AL834130	2	Promoter	N.D.
<i>Homo sapiens</i> mRNA for NTAK <sup>a</sup>	AB005060	2	Promoter	compatible
<i>Homo sapiens</i> mRNA for FLJ00396 protein	AK090474	2	3' region	N.D.
<i>Homo sapiens</i> mRNA for dihydropyrimidinase related protein-3 (DPYSL3) <sup>a</sup>	D78014	2	Promoter	compatible
<i>Homo sapiens</i> hypothetical protein MGC35308	BC034775	2	Exon 1	N.D.
<i>Homo sapiens</i> hypothetical protein MGC33600	BC035022	2	N.D.	N.D.
<i>Homo sapiens</i> growth differentiation factor 7 (GDF7) <sup>a</sup>	AF522369	2	Promoter	compatible
<i>Homo sapiens</i> gene NXN encoding nucleoredoxin	NM_022463	2	N.D.	N.D.
<i>Homo sapiens</i> clone 24649	AF070591	2	3' region	N.D.
<i>Homo sapiens</i> cDNA: FLJ21511	AK025164	2	Promoter	not compatible
<i>Homo sapiens</i> solute carrier family 30, member 10 (SLC30A10) <sup>a</sup>	AK090806	2	Promoter	compatible
<i>Homo sapiens</i> beta-parvin	AF237769	2	Promoter	N.D.
603031612F1 NIH_MGC_115 <i>Homo sapiens</i> cDNA clone IMAGE:5172891	BF489865	2	Promoter	N.D.
<i>Mus musculus</i> adult male spinal cord cDNA, clone:A330088B02	AK079637	1	N.D.	N.D.
<i>Mus musculus</i> 9.5 days embryo parthenogenote cDNA, clone:B130054P17	AK045275	1	N.D.	N.D.
<i>Mus musculus</i> 12 days embryo spinal ganglion cDNA, clone:D130032D18	AK051302	1	N.D.	N.D.
IL5-EN0086-281100-292-f08 EN0086 <i>Homo sapiens</i> cDNA	BF851362	1	N.D.	N.D.
Human receptor tyrosine kinase ligand LERK-7 precursor	U26403	1	Promoter	not compatible
Human solute carrier family 30, member 3 (SLC30A3) <sup>a</sup>	U76010	1	Promoter	compatible
Human platelet-derived growth factor receptor alpha	M21574	1	3' region	N.D.
Human pephBGT-1 betaine-GABA transporter	U27699	1	3' region	N.D.
Human oxytocin mRNA	M25650	1	Promoter	N.D.
Human mRNA for KIAA0222 gene	D86975	1	3' region	N.D.
Human c-kit proto-oncogene (KIT) <sup>a</sup>	X06182	1	Promoter	compatible
Human cell 12-lipoxygenase	M35418	1	Promoter	N.D.
Human bone morphogenetic protein-3 (BMP3) <sup>a</sup>	M22491	1	Promoter	compatible
Human (clone hST3O-1) sialyltransferase	L29555	1	Promoter	N.D.
<i>Homo sapiens</i> , Similar to parathyroid hormone receptor 1	BC031578	1	3' region	N.D.
<i>Homo sapiens</i> , potassium channel, subfamily K, member 13 (KCNK13) <sup>a</sup>	BC012779	1	Promoter	compatible
<i>Homo sapiens</i> , clone MGC:50339	BC043386	1	N.D.	N.D.
<i>Homo sapiens</i> , clone IMAGE:6041910	BC040712	1	Promoter	N.D.
<i>Homo sapiens</i> , clone IMAGE:5590527	BC040874	1	Promoter	N.D.
<i>Homo sapiens</i> Wilms tumor 1	BC032861	1	Promoter	not compatible
<i>Homo sapiens</i> TRALPUSH <sup>a</sup>	AF399708	1	Promoter	compatible
<i>Homo sapiens</i> Sry-related HMG-box protein	AF270652	1	Exon 1	N.D.
<i>Homo sapiens</i> sialyltransferase 4A, transcript variant 2 (SIAT4A) <sup>a</sup>	BC018357	1	Promoter	compatible
<i>Homo sapiens</i> protein tyrosine phosphatase, receptor type, N polypeptide 2	BC034040	1	3' region	N.D.
<i>Homo sapiens</i> prostaglandin E2 receptor	L25124	1	Promoter	N.D.
<i>Homo sapiens</i> polyamine modulated factor-1	AF141310	1	3' region	N.D.
<i>Homo sapiens</i> nuclear receptor subfamily 5, group A, member 1	BC032501	1	3' region	N.D.
<i>Homo sapiens</i> NEL-like 2 (NELL2) <sup>a</sup>	BC020544	1	Promoter	compatible
<i>Homo sapiens</i> mRNA; cDNA DKFZp667I0324	AL832828	1	N.D.	N.D.
<i>Homo sapiens</i> mRNA; cDNA DKFZp564L0472	AL080101	1	3' region	N.D.
<i>Homo sapiens</i> mRNA; cDNA DKFZp564G1482	AL136698	1	Promoter	N.D.
<i>Homo sapiens</i> mRNA, chromosome 1 specific transcript KIAA0495	AB007964	1	Promoter	N.D.
<i>Homo sapiens</i> chromosome 13 open reading frame 21 (C13orf21) <sup>a</sup>	BC029067	1	Promoter	compatible
<i>Homo sapiens</i> mRNA for SOX7 protein <sup>a</sup>	AJ409320	1	Promoter	compatible
<i>Homo sapiens</i> mRNA for nephrosis 2, idiopathic, steroid-resistant (NPHS2) <sup>a</sup>	AJ279254	1	Promoter	compatible
<i>Homo sapiens</i> mRNA for MDC2 alpha, MDC2 beta	AB009671	1	Promoter	N.D.
<i>Homo sapiens</i> mRNA for KIAA0641 protein	AB014541	1	N.D.	N.D.

Table II. Continued

Gene	GenBank accession no.	No. of MCA-RDA clones	Position of MCA-RDA clones	COBRA data
<i>Homo sapiens</i> mRNA for transcription factor 7-like 1 (TCF7L1) <sup>a</sup>	AB031046	1	Promoter	compatible
<i>Homo sapiens</i> mRNA for calmeglin (CLGN) <sup>a</sup>	D86322	1	Promoter	compatible
<i>Homo sapiens</i> mRNA for ADAMTS19 protein <sup>a</sup>	AJ311904	1	Promoter	compatible
<i>Homo sapiens</i> microtubule-associated protein 1B, transcript variant 1	NM_005909	1	Promoter	N.D.
<i>Homo sapiens</i> matrix metalloproteinase-21	AF520613	1	Exon 2	N.D.
<i>Homo sapiens</i> KIAA0534 protein	BC047716	1	Promoter	N.D.
<i>Homo sapiens</i> hypothetical protein MGC49007	BC041175	1	N.D.	N.D.
<i>Homo sapiens</i> hypothetical protein LOC284801	BC036201	1	Promoter	N.D.
<i>Homo sapiens</i> hypothetical protein LOC283887 <sup>a</sup>	BC023651	1	Promoter	compatible
<i>Homo sapiens</i> hypothetical protein BC009980	BC009980	1	Promoter	N.D.
<i>Homo sapiens</i> GATA binding protein 2	BC051342	1	Promoter	not compatible
<i>Homo sapiens</i> forkhead-related transcription factor FREAC-9	AF042832	1	Exon 1	N.D.
<i>Homo sapiens</i> erythroblast macrophage protein EMP	AF084928	1	Promoter	N.D.
<i>Homo sapiens</i> Enah/Vasp-like (EVL) <sup>a</sup>	BC023997	1	Promoter	compatible
<i>Homo sapiens</i> cytokine receptor-like factor 1	BC044634	1	Promoter	N.D.
<i>Homo sapiens</i> cystathionine beta-synthase (CBS) <sup>a</sup>	L14577	1	Promoter	compatible
<i>Homo sapiens</i> clone DNA68818 PSS739	AY358393	1	Promoter	N.D.
<i>Homo sapiens</i> celh-10 homeodomain containing protein	AY336059	1	Exon 1	N.D.
<i>Homo sapiens</i> cDNA FLJ42875	AK124865	1	Promoter	N.D.
<i>Homo sapiens</i> cDNA FLJ41549 <sup>a</sup>	AK123543	1	Promoter	compatible
<i>Homo sapiens</i> cDNA FLJ38293	AK095612	1	Promoter	N.D.
<i>Homo sapiens</i> cDNA FLJ37464 <sup>a</sup>	AK094783	1	Promoter	compatible
<i>Homo sapiens</i> cDNA FLJ33739	AK091058	1	3' region	N.D.
<i>Homo sapiens</i> cDNA FLJ14238	AK024300	1	Promoter	N.D.
<i>Homo sapiens</i> cDNA clone IMAGE:6025756	BC064906	1	Promoter	N.D.
<i>Homo sapiens</i> bridging integrator protein-1	U68485	1	3' region	N.D.
<i>Homo sapiens</i> brain tumor associated protein LRRC4 <sup>a</sup>	AF196976	1	Promoter	compatible
<i>Homo sapiens</i> apoptosis-associated tyrosine kinase, mRNA	BC047378	1	3' region	N.D.
ho64c01.x1 Soares_NFL_T_GBC_S1 <i>Homo sapiens</i> cDNA clone	AW873619	1	Promoter	N.D.
Helix pomatia sulfatase 1 precursor	AF109924	1	Promoter	N.D.
<i>H.sapiens</i> mitogen inducible gene mig-2 (MIG2) <sup>a</sup>	Z24725	1	Promoter	compatible
GENCOURT_8532095 NIH_MGC_113 <i>Homo sapiens</i> cDNA clone	BU899260	1	N.D.	N.D.
EST379664 MAGE resequences, MAGJ <i>Homo sapiens</i> cDNA	AW967589	1	N.D.	N.D.
BX394700 <i>Homo sapiens</i> NEUROBLASTOMA COT 25-NORMALIZED	BX394700	1	Promoter	N.D.
AL545903 <i>Homo sapiens</i> PLACENTA COT 25-NORMALIZED	AL545903	1	Promoter	N.D.
AGENCOURT_8219616 Lupski_sym pathetic_trunk <i>Homo sapiens</i> cDNA clone	BQ722471	1	N.D.	N.D.
AGENCOURT_7546470 NIH_MGC_70 <i>Homo sapiens</i> cDNA clone	BQ218409	1	Promoter	N.D.
7k34c06.x1 NCL_CGAP_Ov18 <i>Homo sapiens</i> cDNA clone IMAGE:3477227	BF058764	1	N.D.	N.D.
602695383F1 NIH_MGC_97 <i>Homo sapiens</i> cDNA clone IMAGE:4827284	BG722892	1	N.D.	N.D.
<i>Homo sapiens</i> mRNA for KIAA0711 protein	AB018254	1	3' region	N.D.
<i>Homo sapiens</i> E2F binding protein	AY152547	1	Exon 1	N.D.
<i>Homo sapiens</i> cDNA FLJ38336	AK095655	1	3' region	N.D.

N.D., not determined. COBRA data indicated that methylation level of the MCA-RDA clones in CRCs positive for *MLH1* methylation was increased (compatible) or not (not compatible) compared with that in CRCs negative for *MLH1* methylation.

<sup>a</sup>Clones analyzed in a test set of samples.

By using COBRA, their CpG methylation status was assessed among the samples used in MCR-RDA. As indicated in Table II, 28 fragments out of 35 were preferentially methylated in the tester DNA, while 7 of them were not.

The methylation status of such 28 fragments was further tested in clinical specimens that had not been used for the initial screening. This test set included eight cancer specimens positive for *MLH1* methylation and the paired normal colon tissue as well as eight cancer specimens negative for *MLH1* methylation (Table I).

The methylation status of each genomic fragment in the clinical specimens is shown color-coded in Figure 1; fragments with a methylation level of  $\geq 10\%$  as determined by COBRA are indicated in red, whereas those with a methylation level of  $< 10\%$  are shown in blue. Most genomic fragments were extensively methylated in most or all of the cancer specimens positive for *MLH1* methylation, but not in those negative for *MLH1* methylation. The difference in CpG

methylation for the MCA-RDA products between the methylated and unmethylated groups of patients was thus confirmed in a distinct test set of CRC specimens.

A more detailed inspection of the data in Figure 1, however, indicates that the MCA-RDA products can be separated into three subgroups on the basis of their methylation profiles. The genomic fragments in the first group (*MIG2* to *NPHS2* in Figure 1) were also methylated in  $\geq 25\%$  of the paired normal colon tissue samples. The fragment corresponding to *MIG2*, for instance, was methylated in all of the *MLH1* methylation-positive cancer specimens and the respective normal tissue. Methylation of these genomic regions thus probably occurred in each patient before the development of CRC and might be related to the aging process.

The genomic fragments in the second group (*BMP3* to *DPYSL3*) were not methylated in normal colon tissue but were methylated in  $\geq 25\%$  of cancer specimens that were negative for *MLH1* methylation. The methylation of these

Gene symbol	CRC specimens positive for <i>MLH1</i> methylation								Normal tissue specimens								CRC specimens negative for <i>MLH1</i> methylation							
	225	263	280	305	318	336	413	416	225	263	280	305	318	336	413	416	238	249	255	278	295	298	307	308
MLH1																								
MIG2																								
SOX7																								
C13orf21																								
FLJ41549																								
PAPLN																								
ADAMTS19																								
FLJ37464																								
LRRC4																								
NFHS2																								
BMP3																								
TRALPUSH																								
SLC30A10																								
EVL																								
DPYSL3																								
MGC29643																								
KCNK13																								
NELL2																								
SLC30A3																								
GDF7																								
NTAK																								
CLGN																								
CBS																								
KIT																								
FBXL7																								
SIAT4A																								
TCF7L1																								
LOC283887																								
IMAGE5728979																								

**Fig. 1.** Gene methylation profiles of CRC specimens. Twenty-eight clones were randomly chosen from the MCA-RDA products of the selected study specimens, and their methylation status (plus that of *MLH1*) was determined by COBRA in CRC specimens positive for the methylation of the *MLH1* promoter ( $n = 8$ ), their paired normal colon tissue samples, and CRC specimens negative for *MLH1* methylation ( $n = 8$ ). Each column represents a clinical specimen (ID numbers are shown), and each row indicates a gene corresponding to an MCA-RDA product. Red box, methylated gene; blue box, unmethylated gene; white box, not examined.

fragments thus appeared to be specific to the cancerous state with a slightly increased prevalence among *MLH1* methylation-positive CRC.

The fragments in the third group (*MGC29643* to *IMAGE5728979*) were methylated in <25% both of normal specimens and of cancer specimens negative for *MLH1* methylation. The methylation of these genes thus appears to be regulated in concert with that of *MLH1*.

#### Analysis of *BMP3*

Among the genomic clones analyzed, we first focused on that corresponding to *BMP3*. *BMP3* is a member of the transforming growth factor- $\beta$  (TGF- $\beta$ ) superfamily of proteins that also includes TGF- $\beta$ 1, TGF- $\beta$ 2, TGF- $\beta$ 3, Mullerian inhibitory substance, *BMP2A*, *BMP2B*, *BMP6*, growth-differentiation factor (*GDF*) 5, *GDF6* and *GDF7* (17,18). Members of this protein superfamily exert inhibitory effects on various human cancers through activation of their cognate receptors and SMAD proteins (19,20). *BMP2*, for instance, induces both the activation of the p38 isoform of mitogen-activated protein kinase and apoptosis in medulloblastoma cells (21). Although little is known of the physiological functions of *BMP3*, it is possible that this protein also possesses antitumor activity and that its expression is epigenetically regulated in cancer cells. Interestingly, Dai *et al.* (22) have recently reported that *BMP3*

promoter is methylated frequently (~50%) in non-small-cell lung carcinoma, which many imply that dysfunction of *BMP3* may be commonly involved in the carcinogenesis of a wide range of human tumors.

The COBRA assay revealed that the MCA-RDA clone corresponding to the promoter region of *BMP3* was methylated in CRC specimens that were positive or negative for *MLH1* methylation (Figures 1 and 2A). Further, as shown in Figure 2B, detailed analysis of the methylation status of the *BMP3* promoter by sequencing of DNA fragments after sodium bisulfite treatment revealed extensive hemi- or biallelic methylation of the promoter in CRC specimens positive for *MLH1* methylation (ID nos 225, 318 and 481) but not in one negative for *MLH1* methylation (ID no. 249). CpG methylation throughout the promoter fragment was also evident in CRC cell lines positive (HCT116) or negative (Caco2) for *MLH1* methylation, but not in the *MLH1* methylation-negative line SW480. Together with the COBRA data in Figure 1, these results suggest that the promoter region of *BMP3* is methylated in all clinical specimens and cell lines positive for methylation of the *MLH1* promoter as well as in some specimens and cell lines negative for *MLH1* methylation.

We then examined whether the epigenetic changes in the *BMP3* promoter affected its transcriptional activity. Quantitative real-time RT-PCR analysis revealed that *BMP3*

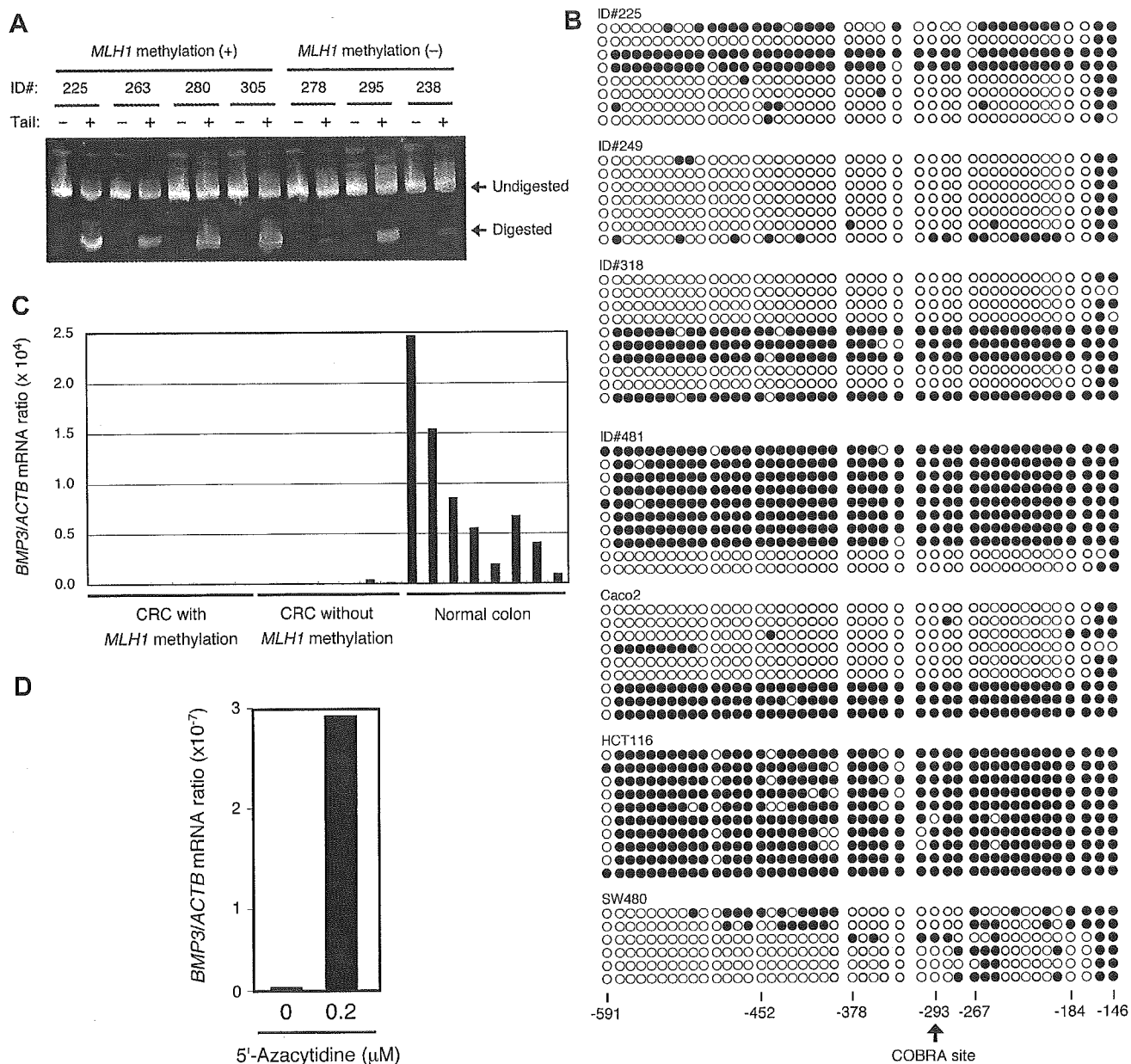


**Fig. 2.** Methylation status of the *BMP3* promoter and *BMP3* expression in CRC specimens. (A) The methylation status of the promoter region of *BMP3* in the indicated clinical specimens was examined by COBRA. Sensitivity of PCR products to digestion with *Tai*I is indicative of methylation of the CpG island examined. (B) Genomic DNA of the indicated clinical specimens and CRC cell lines (Caco2, HCT116 and SW480) was treated with sodium bisulfite, after which the *BMP3* promoter region was amplified by PCR and sequenced. Closed and open circles indicate methylated and unmethylated CpG islands, respectively. The nucleotide positions of the CpG islands (numbered relative to the transcriptional start site) are indicated at the bottom, and the *Tai*I digestion site for COBRA in (A) is shown by the arrow. (C) The level of expression of *BMP3* relative to that of *ACTB* in clinical specimens was determined by quantitative RT-PCR. (D) HCT116 cells were incubated for 72 h with or without 0.2  $\mu$ M of 5'-azacytidine, and were then subjected to RT-PCR analysis for determination of the amount of *BMP3* mRNA relative to that of *ACTB* mRNA.

was transcriptionally silent in CRC specimens positive for *MLH1* methylation (Figure 2C), in which the *BMP3* promoter was also extensively methylated. In contrast, *BMP3* mRNA was abundant in the paired normal colon tissue samples. Although *BMP3* expression was detected in some CRC specimens negative for *MLH1* methylation, the level of expression was greatly reduced compared with that in normal colon tissue. These data thus indicate that *BMP3* transcription is suppressed in most CRCs.

In order to directly examine the relationship between promoter methylation and gene silencing of *BMP3*, HCT116 cells were incubated for 3 days with 5'-azacytidine, an inhibitor of *de novo* methylation of genomic DNA. Interestingly, treatment with 5'-azacytidine markedly induced the amount of *BMP3* mRNA in the cells (Figure 2D) and demethylation of its promoter region as well (data not shown). Therefore, extensive methylation of the *BMP3* promoter region should be directly linked to the suppression of its transcription.

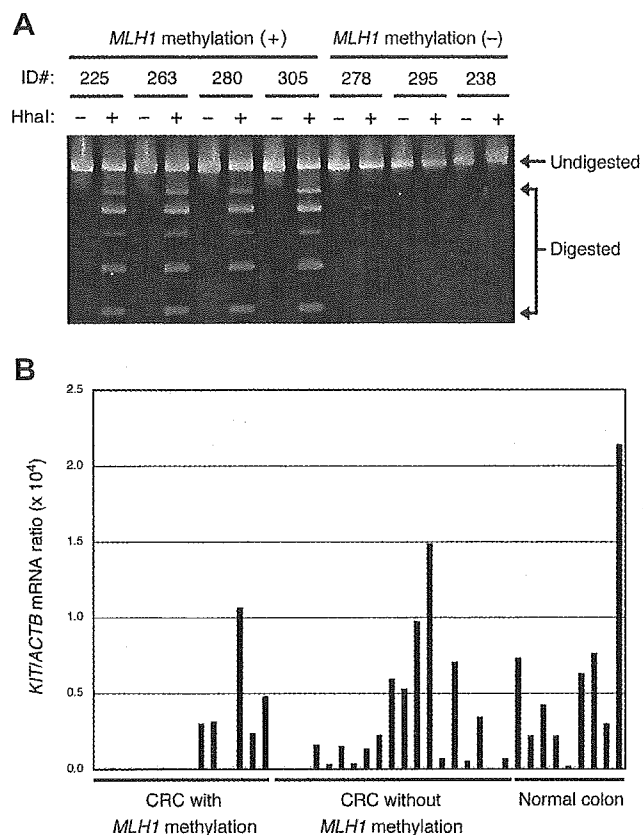


**Fig. 3.** Methylation status of the *KIT* promoter and *KIT* expression in CRC specimens. (A) The methylation status of the promoter region of *KIT* in the indicated clinical specimens was examined by COBRA. Sensitivity of PCR products to digestion with HhaI is indicative of methylation of the CpG island examined. (B) The level of expression of *KIT* relative to that of *ACTB* in clinical specimens was determined by quantitative RT-PCR.

#### Analysis of *KIT*

*KIT* encodes a receptor tyrosine kinase for stem cell factor. Point mutations in *KIT* that increase the kinase activity of the encoded protein have been identified in human gastrointestinal stromal tumors (23), suggestive of a causative role for *KIT* in these tumors. The expression and activation status of *KIT* in CRCs have been unclear, however (24,25). We therefore analyzed the methylation status of the *KIT* promoter region in our samples.

Methylation of the *KIT* promoter was highly restricted to CRC specimens positive for *MLH1* methylation (Figures 1 and 3A). However, the abundance of *KIT* mRNA did not necessarily match the methylation status of the *KIT* promoter. Despite extensive methylation of the promoter in one CRC sample (ID no.77), for instance, the amount of *KIT* mRNA was relatively high ( $KIT/ACTB$  mRNA ratio =  $4.78 \times 10^{-5}$ ), indicating that promoter methylation might not be a major determinant of transcriptional activity. It is possible, however, that our COBRA analysis revealed the methylation status of a CpG site that is not important for *KIT* transcription.

The mean expression level of *KIT* in the *MLH1* methylation-positive CRC specimens [ $KIT/ACTB$  mRNA ratio,  $1.72 \times 10^{-5} \pm 3.02 \times 10^{-5}$  (mean  $\pm$  SD)] was significantly lower than that in normal colon tissue ( $6.03 \times 10^{-5} \pm 6.29 \times 10^{-5}$ ;  $P = 0.038$ , Student's *t*-test). The level of *KIT* expression

in CRCs negative for *MLH1* methylation ( $2.92 \times 10^{-5} \pm 1.61 \times 10^{-5}$ ) was also lower than that in normal colon tissue, but this difference was not significant ( $P = 0.123$ ). It is therefore likely that *KIT* is not overexpressed in CRCs.

#### Discussion

We have screened for genomic fragments whose CpG islands are selectively methylated in CRC specimens positive for methylation of the *MLH1* promoter region. We could readily identify hundreds of genomic fragments with CpG islands that were expected to be differentially methylated between CRCs with or without *MLH1* methylation. Twenty-eight such clones (Table II) were indeed proved to be preferentially methylated in the four CRC specimens positive for *MLH1* methylation compared with the four samples negative for *MLH1* methylation, both of which were used in the original MCA-RDA screening (data not shown).

To verify the selective methylation of these clones, we performed COBRA with a different set of specimens including eight CRCs with *MLH1* methylation and their paired normal tissue samples as well as eight CRCs without *MLH1* methylation. Although all the 28 clones examined were preferentially methylated in the CRC specimens positive for *MLH1* methylation, their methylation profiles among the specimens were not identical, indicating that all CpG methylation observed in MSI-positive CRCs was not specific to this subtype of tumor.

The methylation of certain genomic fragments (14 out of 28 clones examined), however, was highly specific to CRCs that manifested *MLH1* methylation. Almost 50% of the genes were thus methylated in a parallel manner to the CpG methylation of the *MLH1* gene, indicating that a subset of genes is specifically methylated in a subset of CRCs. Our data thus support the existence of CIMP-positive CRCs (14), while it would be mandatory for the better characterization of CIMP-positive tumors to further collect co-methylated genes and to define precisely the hallmark genes for the identification of CIMP (26). It would be interesting to examine whether such clearly defined CIMP is associated with certain clinical manifestations.

Genes corresponding to the co-methylated genomic fragments in our assay included those whose function relates to cell proliferation or differentiation. The predicted structure of *NELL2*, for example, contains epidermal growth factor (EGF)-like repeats (27), which are present in diverse proteins involved in regulation of the cell cycle, cell proliferation, and developmental processes. *NTAK* is a member of the EGF family of proteins and is a ligand and activator of ErbB protein tyrosine kinases (28). In addition, *GDF7* is a member of the TGF- $\beta$  superfamily (18), and *TCF7L1* is highly homologous to *TCF1* which is a target gene of the Wnt- $\beta$ -catenin signaling pathway (29), and which plays an important role in CRC carcinogenesis. Aberrant epigenetic regulation of these genes may thus contribute to the pathogenesis or clinical features of CRCs positive for *MLH1* methylation.

The MCA-RDA method thus proved to be highly effective for the identification of differentially methylated genes among fresh clinical specimens. Given the high fidelity of this approach, it is likely that a large number of genes (or genomic fragments) are methylated in CRCs in concert with methylation of the *MLH1* promoter. Our study provides a basis for further characterization of the molecular pathogenesis of CRCs classified as MSI. Together with the results of other

studies (7,30), it also suggests the possibility of development of a stratification scheme for CRCs based on genome methylation profile.

### Supplementary material

Supplementary material can be found at: <http://www.carcin.oxfordjournals.org/>

### Acknowledgements

This study was supported by a Grant-in-Aid for Third-Term Comprehensive Control Research for Cancer from the Ministry of Health, Labor, and Welfare of Japan, and by a grant for 'High-Tech Research Center' Project for Private Universities: Matching Fund Subsidy (2002–2006) from the Ministry of Education, Culture, Sports, Science, and Technology of Japan.

*Conflict of Interest Statement:* None declared.

### References

- Lengauer, C., Kinzler, K.W. and Vogelstein, B. (1998) Genetic instabilities in human cancers. *Nature*, **396**, 643–649.
- Kinzler, K.W. and Vogelstein, B. (1996) Lessons from hereditary colorectal cancer. *Cell*, **87**, 159–170.
- Ionov, Y., Peinado, M.A., Malkhosyan, S., Shibata, D. and Perucho, M. (1993) Ubiquitous somatic mutations in simple repeated sequences reveal a new mechanism for clonic carcinogenesis. *Nature*, **363**, 558–561.
- Fishel, R., Lescoe, M.K., Rao, M.R., Copeland, N.G., Jenkins, N.A., Garber, J., Kane, M. and Kolodner, R. (1993) The human mutator gene homolog *MSH2* and its association with hereditary non-polyposis colon cancer. *Cell*, **75**, 1027–1038.
- Bronner, C.E., Baker, S.M., Morrison, P.T. et al. (1994) Mutation in the DNA mismatch repair gene homologue *hMLH1* is associated with hereditary non-polyposis colon cancer. *Nature*, **368**, 258–261.
- Papadopoulos, N., Nicolaides, N.C., Wei, Y.F. et al. (1994) Mutation of a mutL homolog in hereditary colon cancer. *Science*, **263**, 1625–1629.
- Toyota, M., Ahuja, N., Ohe-Toyota, M., Herman, J.G., Baylin, S.B. and Issa, J.P. (1999) CpG island methylator phenotype in colorectal cancer. *Proc. Natl Acad. Sci. USA*, **96**, 8681–8686.
- Miyakura, Y., Sugano, K., Konishi, F., Ichikawa, A., Maekawa, M., Shitoh, K., Igarashi, S., Kotake, K., Koyama, Y. and Nagai, H. (2001) Extensive methylation of *hMLH1* promoter region predominates in proximal colon cancer with microsatellite instability. *Gastroenterology*, **121**, 1300–1309.
- Cunningham, J.M., Christensen, E.R., Tester, D.J., Kim, C.Y., Roche, P.C., Burgart, L.J. and Thibodeau, S.N. (1998) Hypermethylation of the *hMLH1* promoter in colon cancer with microsatellite instability. *Cancer Res.*, **58**, 3455–3460.
- Veigl, M.L., Kasturi, L., Olechnowicz, J. et al. (1998) Biallelic inactivation of *hMLH1* by epigenetic gene silencing, a novel mechanism causing human MSI cancers. *Proc. Natl Acad. Sci. USA*, **95**, 8698–8702.
- Koinuma, K., Shitoh, K., Miyakura, Y. et al. (2004) Mutations of BRAF are associated with extensive *hMLH1* promoter methylation in sporadic colorectal carcinomas. *Int. J. Cancer*, **108**, 237–242.
- Wang, L., Cunningham, J.M., Winters, J.L., Guenther, J.C., French, A.J., Boardman, L.A., Burgart, L.J., McDonnell, S.K., Schaid, D.J. and Thibodeau, S.N. (2003) BRAF mutations in colon cancer are not likely attributable to defective DNA mismatch repair. *Cancer Res.*, **63**, 5209–5212.
- Oliveira, C., Pinto, M., Duval, A. et al. (2003) BRAF mutations characterize colon but not gastric cancer with mismatch repair deficiency. *Oncogene*, **22**, 9192–9196.
- Issa, J.P. (2004) Opinion: CpG island methylator phenotype in cancer. *Nat. Rev. Cancer*, **4**, 988–993.
- Toyota, M., Ho, C., Ahuja, N., Jair, K.W., Li, Q., Ohe-Toyota, M., Baylin, S.B. and Issa, J.P. (1999) Identification of differentially methylated sequences in colorectal cancer by methylated CpG island amplification. *Cancer Res.*, **59**, 2307–2312.
- Xiong, Z. and Laird, P.W. (1997) COBRA: a sensitive and quantitative DNA methylation assay. *Nucleic Acids Res.*, **25**, 2532–2534.
- Hogan, B.L. (1996) Bone morphogenetic proteins: multifunctional regulators of vertebrate development. *Genes Dev.*, **10**, 1580–1594.
- Davidson, A.J., Postlethwait, J.H., Yan, Y.L., Beier, D.R., van Doren, C., Foernzler, D., Celeste, A.J., Crosier, K.E. and Crosier, P.S. (1999) Isolation of zebrafish *gdf7* and comparative genetic mapping of genes belonging to the growth/differentiation factor 5, 6, 7 subgroup of the TGF-beta superfamily. *Genome Res.*, **9**, 121–129.
- Miyazono, K., Kusanagi, K. and Inoue, H. (2001) Divergence and convergence of TGF-beta/BMP signaling. *J. Cell. Physiol.*, **187**, 265–276.
- Bottlinger, E.P., Jakubczak, J.L., Haines, D.C., Bagnall, K. and Wakefield, L.M. (1997) Transgenic mice overexpressing a dominant-negative mutant type II transforming growth factor beta receptor show enhanced tumorigenesis in the mammary gland and lung in response to the carcinogen 7,12-dimethylbenz[*a*]anthracene. *Cancer Res.*, **57**, 5564–5570.
- Hallahan, A.R., Pritchard, J.I., Chandraratna, R.A., Ellenbogen, R.G., Geyer, J.R., Overland, R.P., Strand, A.D., Tapscott, S.J. and Olson, J.M. (2003) BMP-2 mediates retinoid-induced apoptosis in medulloblastoma cells through a paracrine effect. *Nat. Med.*, **9**, 1033–1038.
- Dai, Z., Popkie, A.P., Zhu, W.G. et al. (2004) Bone morphogenetic protein 3B silencing in non-small-cell lung cancer. *Oncogene*, **23**, 3521–3529.
- Hirota, S., Iizaki, K., Moriyama, Y. et al. (1998) Gain-of-function mutations of *c-kit* in human gastrointestinal stromal tumors. *Science*, **279**, 577–580.
- Bellone, G., Silvestri, S., Artusio, E., Tibaudi, D., Turletti, A., Geuna, M., Giachino, C., Valente, G., Emanuelli, G. and Rodeck, U. (1997) Growth stimulation of colorectal carcinoma cells via the *c-kit* receptor is inhibited by TGF-beta 1. *J. Cell. Physiol.*, **172**, 1–11.
- Sammarco, I., Capurso, G., Coppola, L. et al. (2004) Expression of the proto-oncogene *c-KIT* in normal and tumor tissues from colorectal carcinoma patients. *Int. J. Colorectal Dis.*, **19**, 545–553.
- Yamashita, K., Dai, T., Dai, Y., Yamamoto, F. and Perucho, M. (2003) Genetics supersedes epigenetics in colon cancer phenotype. *Cancer Cell*, **4**, 121–131.
- Watanabe, T.K., Katagiri, T., Suzuki, M., Shimizu, F., Fujiwara, T., Kanemoto, N., Nakamura, Y., Hirai, Y., Maekawa, H. and Takahashi, E. (1996) Cloning and characterization of two novel human cDNAs (*NELL1* and *NELL2*) encoding proteins with six EGF-like repeats. *Genomics*, **38**, 273–276.
- Higashiyama, S., Horikawa, M., Yamada, K. et al. (1997) A novel brain-derived member of the epidermal growth factor family that interacts with ErbB3 and ErbB4. *J. Biochem.*, **122**, 675–680.
- Castrop, J., van Norren, K. and Clevers, H. (1992) A gene family of HMG-box transcription factors with homology to TCF-1. *Nucleic Acids Res.*, **20**, 611.
- Toyota, M., Ohe-Toyota, M., Ahuja, N. and Issa, J.P. (2000) Distinct genetic profiles in colorectal tumors with or without the CpG island methylator phenotype. *Proc. Natl Acad. Sci. USA*, **97**, 710–715.

Received April 29, 2005; revised July 10, 2005; accepted July 12, 2005

## Retroviral expression screening of oncogenes in pancreatic ductal carcinoma

Hiroyuki Kisanuki <sup>a</sup>, Young Lim Choi <sup>a</sup>, Tomoaki Wada <sup>a</sup>, Ryoza Moriuchi <sup>b</sup>,  
Shin-ichiro Fujiwara <sup>a</sup>, Ruri Kaneda <sup>a</sup>, Koji Koinuma <sup>a</sup>, Madoka Ishikawa <sup>a</sup>,  
Shuji Takada <sup>a</sup>, Yoshihiro Yamashita <sup>a</sup>, Hiroyuki Mano <sup>a,c,\*</sup>

<sup>a</sup> Division of Functional Genomics, Jichi Medical School, 3311-1 Yakushiji, Kawachigun, Tochigi 329-0498, Japan

<sup>b</sup> Department of Molecular Microbiology and Immunology, Nagasaki University Graduate School of Medicine, Nagasaki, Japan

<sup>c</sup> CREST, Japan Science and Technology Agency, Saitama, Japan

Received 4 March 2005; received in revised form 3 May 2005; accepted 10 May 2005

Available online 25 August 2005

### Abstract

Pancreatic ductal carcinoma (PDC) remains one of the most intractable malignancies in humans. In order to clarify the molecular events underlying the carcinogenesis in PDC, we constructed a retroviral cDNA expression library from a PDC cell line, and used it to screen transforming genes in PDC by a focus formation assay with mouse 3T3 fibroblasts. We could obtain a total of 30 transformed cell foci in the screening, and one of the cDNA inserts harvested from such cell clones turned out to encode a wild-type human ARAF1. Unexpectedly, a long terminal repeat-driven overexpression of *ARAF1* mRNA was confirmed to induce transformed foci in fibroblasts. The oncogenic potential of ARAF1 was examined by injecting the transformed fibroblasts into athymic nude mice. Importantly, *ARAF1* mRNA was highly expressed in pancreatic ductal cell specimens purified from patients with PDC. These results have unveiled the transforming potential of ARAF1 protein, and also suggest that quantity of intracellular ARAF1 may be important in carcinogenesis of various human cancers.

© 2005 Elsevier Ltd. All rights reserved.

**Keywords:** Pancreatic ductal cell carcinoma; Retrovirus; ARAF1; cDNA library; Oncogene

### 1. Introduction

Pancreatic ductal carcinoma (PDC) originates from pancreatic ductal cells, and is one of the most intractable malignancies in humans [1,2]. Effective therapy for PDC is hampered by the lack of specific clinical symptoms. At the time of diagnosis, most patients are no longer candidates for surgical resection, and, even in individuals who do undergo such surgery, the 5-year survival rate is only 20–30% [1].

Vast efforts have been made to elucidate molecular events responsible for the carcinogenesis of PDC. Mutations of *TP53* gene can be, for instance, found in PDC specimens [3], and in the intraductal *in situ* regions as well [4]. Similarly, inactivation has been found for other tumour-suppressor genes, such as *DPC*, *RB1* and *p16* [5].

As for oncogenes, activating mutations in the *KRAS2* gene has been reported to be frequently associated with PDC [6]. The same *KRAS2* mutations could be, however, found in the samples for chronic pancreatitis [7], making their pathogenetic role uncertain. Additionally, an increased telomerase activity was shown to be present only in PDC, but not in nonmalignant pancreatic disorders [8]. Again, however, others could detect an elevated telomerase activity in chronic pancreatitis and normal

\* Corresponding author. Tel.: +81 285 58 7449; fax: +81 285 44 7322.

E-mail address: hmano@jichi.ac.jp (H. Mano).

pancreas [9]. Therefore, it is yet to be revealed which transforming genes truly promote a clonal growth of pancreatic ductal cells.

For an efficient isolation of tumour-promoting genes in PDC, it would be desirable to conduct functional screening based on transforming ability. Focus formation assays with mouse 3T3 fibroblasts have been highly successful for the identification of oncogenes in human cancer [10]. In such screening, genomic DNA is isolated from cancer specimens, and used to transfect 3T3 cells to obtain transformed cell foci. It should be noted, however, that, since expression of any genes in these experiments are driven by their own promoters/enhancers, oncogenes in PDC can exert their effects in 3T3 cells only when the promoter/enhancer regions of such genes are active in fibroblasts, which is not always guaranteed.

To ensure the sufficient expression of cDNAs in 3T3 cells, their transcription should be regulated by an exogenous promoter fragment. We have therefore constructed a retroviral cDNA expression library from a PDC cell line, MiaPaCa-2, which was used to infect 3T3 cells. In the preparation of cDNA library, we further took advantage of the SMART polymerase chain reaction (PCR) system (Clontech, Palo Alto, CA), which preferentially amplifies full-length cDNAs. A focus formation assay with the library resulted in an identification of a transforming *ARAF1* gene.

## 2. Materials and methods

### 2.1. Cells and culture

MiaPaCa-2, Capan-2, PANC-1, 3T3, and BOSC23 [11] cell lines were obtained from American Type Culture Collection, and maintained in Dulbecco's modified Eagle medium/F12 (DMEM/F12; Invitrogen, Carlsbad, CA) containing 10% fetal bovine serum (Invitrogen) and 2 mM L-glutamine.

The fresh clinical specimens were obtained from patients who gave informed consent, and the study was approved by the institutional review board of Jichi Medical School. Cells were collected from the pancreatic juice by centrifugation, labeled with anti-MUC1 antibody [12] (Novocastra Laboratories, Newcastle upon Tyne, UK), and subjected to chromatography on a miniMACS magnetic cell separation column (Miltenyi Biotec, Auburn, CA) [13]. The purity of the resultant MUC1<sup>+</sup> cell fraction was confirmed by staining with Wright Giemsa solutions and microscopy examination for each case (data not shown).

### 2.2. Retrovirus library construction

Total RNA was extracted from MiaPaCa-2 cells by an RNeasy Mini column with RNase-free DNase (Qiagen,

Valencia, CA), and the first strand cDNA was synthesized by PowerScript reverse transcriptase (Clontech) with SMART IIA oligonucleotide and CDS primer IIA (both from Clontech). The cDNAs were then amplified for 12 cycles with 5' PCR primer IIA according to the instruction of the SMART PCR cDNA synthesis kit (Clontech) except a substitution of LA Taq polymerase (Takara Bio, Shiga, Japan) for Advantage 2 DNA polymerase provided with the kit. Resultant cDNAs were treated with proteinase K, blunt-ended by T4 DNA polymerase, and ligated to the BstXI-adaptor (Invitrogen). Unbound adaptors were removed through the cDNA size fractionation column (Invitrogen), and the cDNAs were finally ligated to the pMXS retroviral plasmid (a kind gift of Dr. T. Kitamura at Institute of Medical Science, University of Tokyo) [14] digested with BstXI. The pMXS-cDNA plasmids were introduced into ElectroMax DH10B cells (Invitrogen) with electroporation.

### 2.3. Focus formation assay

Generation of recombinant retroviral library and focus formation assay was conducted as described previously [15]. Briefly, BOSC23 cells were transfected with Lipfectamin reagent (Invitrogen) and 2 µg of retroviral plasmid together with 0.5 µg of pGP plasmid 0.5 µg of pE-eco plasmid (both from Takara Bio). Two days after the transfection, polybrene (Sigma, St. Louis, MI) was added to the culture supernatant at a concentration of 4 µg/ml, and the supernatant was subsequently used to infect 3T3 cells for 48 h. For the focus formation assay, the culture medium of 3T3 cells was then changed to DMEM-high glucose (Invitrogen) supplemented with 5% calf serum and 2 mM L-glutamine. Transformed foci were picked up after 3 weeks of culture. Genomic DNA was extracted from each transformed focus, and was subjected to PCR with 5' PCR primer IIA (Clontech) and LA Taq polymerase for 50 cycles of 98 °C for 20 s and 68 °C for 6 min. Amplified genome fragments were purified for nucleotide sequencing. For tumorigenicity assay in nude mice, transformed 3T3 cells were injected into each shoulder of nu/nu Balb-c mice (6 weeks old). Tumour formation was assessed after 4 weeks.

### 2.4. "Real-time" RT-PCR

Portions of oligo(dT)-primed cDNA were subjected to PCR with a QuantiTect SYBR Green PCR Kit (Qiagen). The amplification protocol was comprised of incubations at 94 °C for 15 s, 57 °C for 30 s, and 72 °C for 60 s. Incorporation of the SYBR Green dye into PCR products was monitored in real time with an ABI PRISM 7900HT sequence detection system (PE Applied Biosystems, Foster City, CA), thereby allowing determination of the threshold cycle ( $C_T$ ) at which exponential amplification of products



begins. The  $C_T$  values for cDNAs corresponding to the  $\beta$ -actin gene (*ACTB*) and to the *ARAF1* gene were used to calculate the abundance of the latter mRNA relative to that of the former. The oligonucleotide primers for PCR were as follows: 5'-CCATCATGAAGTGTGACGTGG-3' and 5'-GT-CCGCCTAGAAGCATTGCG-3' for *ACTB*, and 5'-ACTACCTCCATGCCAAGAACATCA-3' and 5'-GACGTCTGACTGGAAGCTGTAGGG-3' for *ARAF1*.

### 3. Results

#### 3.1. Screening with focus formation assay

From mRNA of MiaPaCa-2 cells, full-length cDNAs were selectively amplified and ligated to a retroviral vector pMXS. We could obtain a total of  $2.1 \times 10^6$  colony forming units (cfu) of independent plasmid clones. Thirty clones were randomly selected from the library, and examined for the incorporated cDNAs. Twenty-seven (90%) out of the 30 clones contained inserts with an average length of 2.05 kbp.

By introducing the plasmid DNA into a packaging cell line, we generated a recombinant ecotropic retrovirus library that was subsequently used to infect mouse 3T3 fibroblasts. Infection experiments were repeated for a total of 6 times. After 3 weeks of culture, 30 transformed foci were observed (Fig. 1(b)). No foci could be found among the cells infected with an empty virus (Fig. 1(a)), while numerous foci were easily identified

in the cells infected with a virus expressing v-Ras oncoprotein (Fig. 1(c)).

Each focus was isolated, expanded independently, and was subject to the extraction of genomic DNA. We then tried to recover retroviral inserts from the genomic DNA by PCR amplification with the primer used originally to amplify the cDNAs in the construction of the library. In most cases, two to three DNA fragments were recovered from each genome (Fig. 2(a)), implying a multiple retroviral infection on the recipient 3T3 cells.

We obtained a total of 56 cDNA fragments by PCR, all of which were subjected to nucleotide sequencing from both ends. Screening of the cDNA sequences against human genome sequence database assembled as of July 2003 by the Genome Bioinformatics Group of the University of California at Santa Cruz (<http://genome.ucsc.edu>) revealed that the 56 fragments correspond to 13 independent genes, eleven of which could be matched at >95% identity to the human genome sequence (Table 1). Among the 11 genes, 7 of them were known genes while the rest 4 were unknown. Each cDNA clone was ligated to pMXS in both directions, and a recombinant retrovirus was generated from each resultant plasmid. Transforming ability of the cDNAs was thus confirmed by a focus formation assay with the recombinant virus.

Focus formation assays were conducted for the 26 independent viruses (all 13 independent genes for both directions), and one of them, expressing ARAF1 protein (GenBank accession number, NM\_001654), gave transformed foci in repeated experiments. ARAF1 belongs to

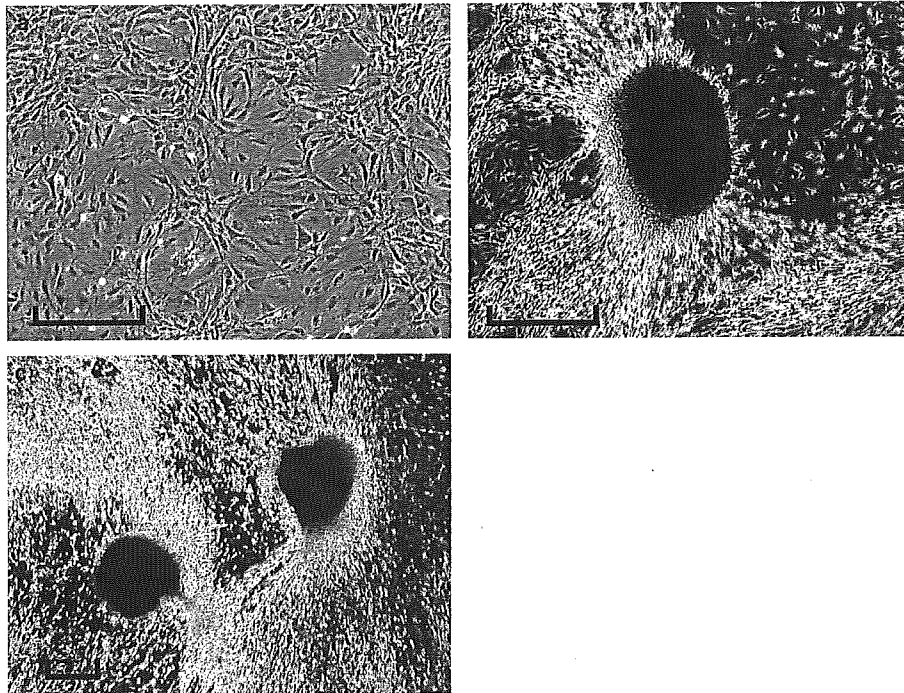


Fig. 1. Focus formation assay with retroviral library. Mouse 3T3 cells were infected with (a) an empty virus, (b) retroviruses from the MiaPaCa-2 library, or (c) a retrovirus expressing v-Ras as a positive control. Pictures were taken after 3 weeks of culture. Scale bar, 100  $\mu$ m.

Table 1  
cDNAs isolated from 3T3 transformants

Clone #	Gene symbol	GenBank number	Covering full ORF
1	Unknown	AK026325	ND
2	No homologues sequences	ND	ND
3	Unknown	AF318370	Yes
4	PITPNM1	NM_004910	No
5	Unknown	BC022099	Yes
6	DECR2	NM_020664	Yes
7	ARAF1	NM_001654	Yes
8	BCLG	NM_138724	No
9	No homologues sequences	ND	ND
10	Unknown	AL607122	ND
11	JAG1	NM_000214	Yes
12	MRPL43	NM_176792	Yes
13	PLOD3	NM_001084	No

ORF, open reading frame; ND, not determined.

the RAF family of serine/threonine kinases, and phosphorylates MEK1 [16]. It had not been known whether an overexpression of wild ARAF1 protein has a transforming activity.

### 3.2. ARAF1 as an oncogene

We thus determined the whole nucleotide sequence of our ARAF1 cDNA (cDNA clone ID #7). The sequence is 2441 bp, and contains an open reading frame (spanning nucleotide position 126–1943) encoding a protein of 606 amino acids, which is identical to ARAF1 (Fig. 2(b)). Within the protein-coding region, there is only one nucleotide mutation compared to the published ARAF1 cDNA sequence; a “T” at nucleotide position 1550 in the reported sequence (NM\_001654) is replaced with a “C” in our sequence. The codon sequence “TTG” at the amino acid position 450 of ARAF1 is thus changed to “CTG” in our cDNA. However, both codons encode the same leucine residue, and thus the mutation does not affect the protein sequence.

To confirm that mere overexpression of wild ARAF1 protein has a transforming activity, we repeated the focus formation assay with the retrovirus generated from our ARAF1 cDNA. As shown in Fig. 2(c), the recombinant virus reproducibly induced transformed foci (30–50 foci per microgram of the input plasmid) in the recipient 3T3 cells. The transforming ability of ARAF1 was also tested by the tumorigenicity assay with athymic nude mice. The 3T3 cells infected with the empty virus or retrovirus expressing ARAF1 or v-Ras were inoculated subcutaneously into nude mice. As shown in Fig. 2(d), tumour formation was observed in all mice for the latter 2 cases, arguing that ARAF1 has oncogenic potential.

### 3.3. Expression of ARAF1 in PDC

We finally measured the expression level of ARAF1 mRNA in PDC by the quantitative real-time reverse

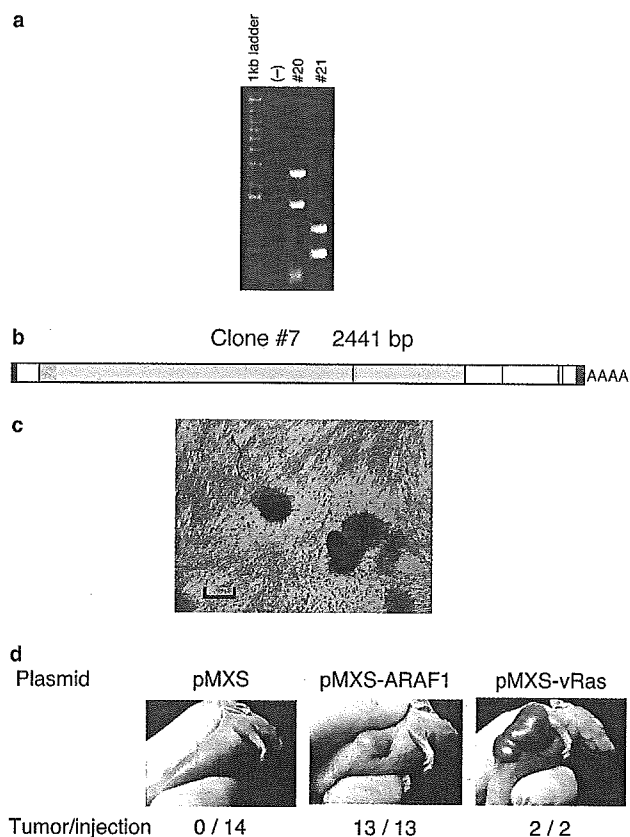


Fig. 2. Identification of the transforming ARAF1 gene. (a) Genomic DNAs isolated from the transformed foci (cell clone ID #20 and #21) were subjected to PCR. A PCR without DNA template was also conducted as a negative control (–). DNA size markers (1 kb DNA ladder; Invitrogen) are electrophoresed at the left. (b) A 3T3 clone yielded a PCR product of 2441 bp long (cDNA clone ID #7). The cDNA has a protein-coding region (gray) for 606 amino acids that was identical to human ARAF1 protein. Nucleotides that did not match the published ARAF1 cDNA are indicated by red lines. (c) Our ARAF1 cDNA was ligated to pMXS, and used to generate recombinant virus. Infection with the virus induced multiple transformed foci in 3T3 cells. Scale bar, 100 µm. (d) 3T3 cells ( $5 \times 10^5$ ) were cultured for two days with retrovirus made from pMXS, pMXS-ARAF1 or pMXS-vRas plasmid, and were injected subcutaneously into nu/nu mice. Tumour formation was examined after 4 weeks.

transcription (RT)-PCR method. As shown in Fig. 3, all 3 PDC cell lines express similar amounts of ARAF1 mRNA. In addition, we quantified ARAF1 mRNA in human clinical specimens. Pancreatic juice from patients with PDC contains cancer cells (transformed ductal cells) in addition to normal ductal cells and blood cells. The former two fractions were purified, by an affinity column for MUC1 surface protein [12], from pancreatic juice of PDC patients ( $n = 14$ ). Such purified fractions should be highly enriched for PDC cells [13]. Similar MUC1-positive fractions were also purified from the pancreatic juice of healthy individuals ( $n = 7$ ). Quantification of ARAF1 mRNA revealed that its mRNA level was highly elevated in six out of the 14 patient, but not in the specimens from healthy individuals. These data

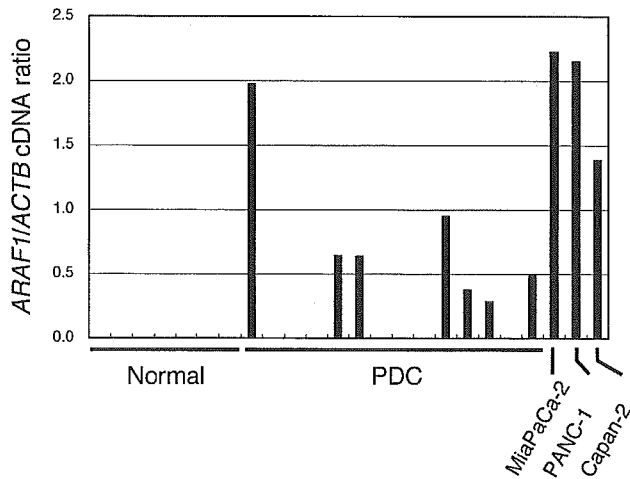


Fig. 3. Quantification of *ARAF1* mRNA. Complementary DNA was prepared from PDC cell lines (MiaPaCa-2, PANC-1 and Capan-2) or MUC1<sup>+</sup> ductal cell preparations purified from healthy individuals (Normal) or patients with PDC, and were then subjected to real-time RT-PCR analysis with primers specific for the *ARAF1* or *ACTB* genes. The ratio of the abundance of *ARAF1* mRNA to that of *ACTB* mRNA was calculated as  $2^n$ , where  $n$  is the  $C_T$  value for *ACTB* cDNA minus the  $C_T$  value for *ARAF1* cDNA.

indicate that the transcription of *ARAF1* is selectively activated in PDC cells.

#### 4. Discussion

In this manuscript, we have constructed a retroviral cDNA expression library of PDC. Since 90% (27/30) of the viral plasmids carried cDNA inserts and since the overall clone number was >2 millions, our library should cover nearly all transcriptome in MiaPaCa-2 cells.

RAF family is composed of RAF1, ARAF1 and BRAF in humans. All these serine/threonine kinases are believed to act downstream of RAS-family proteins, and to phosphorylate and regulate downstream MAP kinase kinases (MAPKKs). Many studies have revealed transforming potentials of RAF family proteins. RAF was originally identified as a cellular homologue of viral oncoprotein, v-Raf [17]. Deletion of amino-terminal regions unmasks the transforming ability of RAF1 [18] and ARAF1 [19]. On the other hand, somatic point mutations have been found in the *BRAF* gene among clinical specimens of colorectal carcinoma [20]. Such mutations were shown to induce transforming activity in BRAF protein. In contrast to *BRAF*, somatic point mutations are rarely found in *ARAF1* gene [21].

Overexpression of wild forms of RAF1 or BRAF failed to exert a transforming activity [18,20]. Although deletion/truncation of amino terminal regions of ARAF1 induced transformed foci in 3T3 fibroblasts [22] and abrogated cytokine-dependency in hematopoietic cells [19], it has not been tested whether wild ARAF1 protein has transforming potential. In this

manuscript, however, it was unexpectedly revealed that a long terminal repeat-driven expression of ARAF1 induces transformed foci in 3T3 cells, which subsequently generated tumours in immunocompromised mice. Therefore, it has been unveiled here that an overexpression of wild ARAF1 is directly linked with cellular transformation process.

These data also indicate the importance of measuring protein/mRNA amounts of ARAF1 in various human cancers. In this context, it was interesting to find a high expression of *ARAF1* mRNA in fresh clinical specimens of PDC. Our findings shed new light on the understanding of RAF family kinases, and open up the possibility that ARAF is involved in carcinogenesis in human cancers through a previously unexpected mechanism.

#### Conflict of interest statement

None declared.

#### Acknowledgments

This work was supported in part by a grant for Third-Term Comprehensive Control Research for Cancer from the Ministry of Health, Labor, and Welfare of Japan; and a grant for "High-Tech Research Center" Project for Private Universities: Matching Fund Subsidy (2002–2006) from the Ministry of Education, Culture, Sports, Science, and Technology of Japan.

#### References

- Bornman PC, Beckingham IJ. Pancreatic tumours. *Br Med J* 2001, **322**, 721–723.
- Rosewicz S, Wiedenmann B. Pancreatic carcinoma. *Lancet* 1997, **349**, 485–489.
- Goggins M, Kern SE, Offerhaus JA, et al. Progress in cancer genetics: lessons from pancreatic cancer. *Ann Oncol* 1999, **10**(Suppl. 4), 4–8.
- Barton CM, Staddon SL, Hughes CM, et al. Abnormalities of the p53 tumour suppressor gene in human pancreatic cancer. *Br J Cancer* 1991, **64**, 1076–1082.
- Bramhall SR. The use of molecular technology in the differentiation of pancreatic cancer and chronic pancreatitis. *Int J Pancreatol* 1998, **23**, 83–100.
- Tada M, Omata M, Ohto M. Clinical application of ras gene mutation for diagnosis of pancreatic adenocarcinoma. *Gastroenterology* 1991, **100**, 233–238.
- Yanagisawa A, Ohtake K, Ohashi K, et al. Frequent c-Ki-ras oncogene activation in mucous cell hyperplasias of pancreas suffering from chronic inflammation. *Cancer Res* 1993, **53**, 953–956.
- Hiyama E, Kodama T, Shinbara K, et al. Telomerase activity is detected in pancreatic cancer but not in benign tumours. *Cancer Res* 1997, **57**, 326–331.
- Uehara H, Nakaizumi A, Tatsuta M, et al. Diagnosis of pancreatic cancer by detecting telomerase activity in pancreatic

- juice: comparison with K-ras mutations. *Am J Gastroenterol* 1999, **94**, 2513–2518.
10. Aaronson SA. Growth factors and cancer. *Science* 1991, **254**, 1146–1153.
  11. Pear WS, Nolan GP, Scott ML, et al. Production of high-titer helper-free retroviruses by transient transfection. *Proc Natl Acad Sci USA* 1993, **90**, 8392–8396.
  12. Terada T, Ohta T, Sasaki M, et al. Expression of MUC apomucins in normal pancreas and pancreatic tumours. *J Pathol* 1996, **180**, 160–165.
  13. Yoshida K, Ueno S, Iwao T, et al. Screening of genes specifically activated in the pancreatic juice ductal cells from the patients with pancreatic ductal carcinoma. *Cancer Sci* 2003, **94**, 263–270.
  14. Onishi M, Kinoshita S, Morikawa Y, et al. Applications of retrovirus-mediated expression cloning. *Exp Hematol* 1996, **24**, 324–329.
  15. Yoshizuka N, Moriuchi R, Mori T, et al. An alternative transcript derived from the trio locus encodes a guanosine nucleotide exchange factor with mouse cell-transforming potential. *J Biol Chem* 2004, **279**, 43998–44004.
  16. Wu X, Noh SJ, Zhou G, et al. Selective activation of MEK1 but not MEK2 by A-Raf from epidermal growth factor-stimulated Hela cells. *J Biol Chem* 1996, **271**, 3265–3271.
  17. Bonner TI, Kerby SB, Suttrave P, et al. Structure and biological activity of human homologs of the raf/mil oncogene. *Mol Cell Biol* 1985, **5**, 1400–1407.
  18. Ishikawa F, Sakai R, Ochiai M, et al. Identification of a transforming activity suppressing sequence in the c-raf oncogene. *Oncogene* 1988, **3**, 653–658.
  19. Hoyle PE, Moye PW, Steelman LS, et al. Differential abilities of the Raf family of protein kinases to abrogate cytokine dependency and prevent apoptosis in murine hematopoietic cells by a MEK1-dependent mechanism. *Leukemia* 2000, **14**, 642–656.
  20. Davies H, Bignell GR, Cox C, et al. Mutations of the BRAF gene in human cancer. *Nature* 2002, **417**, 949–954.
  21. Lee JW, Soung YH, Kim SY, et al. Mutational analysis of the ARAF gene in human cancers. *APMIS* 2005, **113**, 54–57.
  22. Beck TW, Huleihel M, Gunnell M, et al. The complete coding sequence of the human A-raf-1 oncogene and transforming activity of a human A-raf carrying retrovirus. *Nucleic Acids Res* 1987, **15**, 595–609.

## Research Article

# Regulation of *Amh* during sex determination in chickens: *Sox* gene expression in male and female gonads

S. Takada<sup>a,b</sup>, H. Mano<sup>b</sup> and P. Koopman<sup>a,\*</sup>

<sup>a</sup> Institute for Molecular Bioscience, The University of Queensland, Brisbane, Queensland 4072 (Australia),  
Fax: +61 7 3346 2101, e-mail: p.koopman@imb.uq.edu.au

<sup>b</sup> Division of Functional Genomics, Jichi Medical School, 3311-1 Yakushiji, Minamikawachimachi, Kawachigun,  
Tochigi 329-0498 (Japan)

Received 18 June 2005; received after revision 22 June 2005; accepted 27 June 2005  
Online First 26 August 2005

**Abstract.** During mammalian sexual development, the SOX9 transcription factor up-regulates expression of the gene encoding anti-Müllerian hormone (AMH), but in chickens, *Sox9* gene expression reportedly occurs after the onset of *Amh* expression. Here, we examined expression of the related gene *Sox8* in chicken embryonic gonads during the sex-determining period. We found that *cSox8* is expressed at similar levels in both sexes at embryonic day 6 and 7, and only at the anterior tip of the

gonad, suggesting that SOX8 is not responsible for the sex-specific increase in *cAmh* gene expression at these stages. We also found that several other chicken *Sox* genes (*cSox3*, *cSox4* and *cSox11*) are expressed in embryonic gonads, but at similar levels in both sexes. Our data suggest that the molecular mechanisms involved in the regulation of *Amh* genes of mouse and chicken are not conserved, despite similar patterns of *Amh* expression in both species.

**Key words.** Sex determination; *Amh*; chicken; testis.

Even though molecular mechanisms of patterning and morphogenesis are surprisingly well conserved during metazoan evolution, mechanisms governing sex determination and gonadal development are diverse, even among vertebrates. In mammals, the heterogametic pairing of sex chromosomes (XY) results in male development. The mouse and human sex-determining gene, *Sry/SRY* (sex-determining region on Y chromosome), has been identified [1, 2] and is known to cause the bipotential gonad to differentiate into a testis [3]. However, *Sry* is not a conserved sex-determining gene as it exists only in mammals [4–7]. In contrast to mammals, in birds males are homogametic (ZZ) and females are heterogametic for the sex chromosomes (ZW). Whether avian sex is

determined by a master female-determining gene on the W chromosome or by Z chromosome gene dosage is still unclear [8].

There are reports for the mouse that several genes are expressed predominantly in the developing testis but not in the ovary and, therefore, are likely to be important for male sex determination and differentiation. Some of these genes, such as *Amh* (anti-Müllerian hormone) and *Sox9* [9–12] are expressed similarly in mouse and chicken gonads, suggesting that there could be some degree of similarity between the molecular pathways and sexual development in chicken and mouse. However, some differences are evident. For example, *Sfl* (steroidogenic factor 1) and *Gata4* are predominantly expressed in the male gonad in mice [13, 14], while in chicken expression levels of both genes are similar between male and female gonads [12, 15].

\* Corresponding author.

*Sox* genes represent a family related by the *Sry*-type high-mobility group (HMG) box, and function as transcription factors in various developmental processes through binding to a conserved core DNA sequence [16]. Twenty *Sox* genes have been identified in mouse and human, and are classified by their HMG box sequences into subgroups A–H [17, 18]. The expression pattern of each gene tends to be conserved in mouse and chicken. Among them, *Sox9* (group E) is known to act as a sex-determining gene. Mutations of human *SOX9* cause campomelic dysplasia, a severe skeletal malformation syndrome associated in most cases with XY sex reversal [19, 20], and ectopic expression of *Sox9* in XX mouse fetal gonads induces testis formation [21].

AMH plays an important role in inducing the regression of the Müllerian ducts in males, which normally give rise to the uterus, oviducts, upper vagina and fallopian tubes in females [22]. Analysis of mouse and human *Amh* gene regulation has uncovered several factors important for modulating *Amh* expression. For example, SF1 up-regulates *Amh* expression by cooperative interaction with WT1 [23], GATA-4 [24], SOX9 [25] and SOX8 [26]. Mice mutant for the SOX-binding site or the SF1-binding site in the *Amh* promoter revealed that SOX proteins are essential for *Amh* expression, while SF1 enhances the final expression level [27]. Oréal et al. [28] were the first to describe the chicken *Amh* promoter and showed that it has little overall homology with the mouse *Amh* promoter, but contains two putative SOX-binding sites and one SF1-binding site, suggesting that the mouse and chicken *Amh* promoters are similarly regulated. However, chicken *Sox9* is expressed too late to be a *cAmh* regulator [28, 29], but another SOX protein might substitute for SOX9 and, together with SF1, regulate *cAmh* expression.

Previously, we hypothesized that SOX8 might be a candidate transcription factor for regulating the chicken *Amh* gene [26, 30]. Mouse *Sox8* is expressed male specifically during gonad development. Its expression starts prior to the onset of *Amh* gene expression, and encodes a protein product that can up-regulate mouse *Amh* together with SF1 in vitro [26]. Group E *Sox* genes, consisting of *Sox8*, *Sox9* and *Sox10*, show moderate levels of amino acid similarity and have similar genomic organization, suggesting that group E *Sox* genes may originate from one ancestral gene [31]. Although expression patterns of *Sox9* and *Sox10* overlap to a limited extent [32, 33], expression of *Sox8* overlaps substantially with expression of *Sox9* [31, 32] and to a lesser extent, *Sox10* [33, 31]. This fact suggests that there is some functional redundancy between SOX8 and SOX9, similar to that published for SOX1, SOX2 and SOX3 in lens formation [34], L-SOX5 and SOX6 in cartilage formation [35] and SOX7, SOX17 and SOX18 in vasculogenesis [36–38].

In this study, we analyzed the expression patterns of chicken *Sox8* in developing gonads during the sex-deter-

mining window. If *cSox8* contributes to *cAmh* gene expression, one would expect to find *cSox8* predominantly expressed in the embryonic testis and prior to the onset of *cAmh*. We found this not to be the case, suggesting that SOX8 is not responsible for sex-specific expression of *cAmh* in chicken. We also tested the expression patterns of several other *cSox* genes which are expressed in embryonic testis, and similarly found that they were not expressed male specifically.

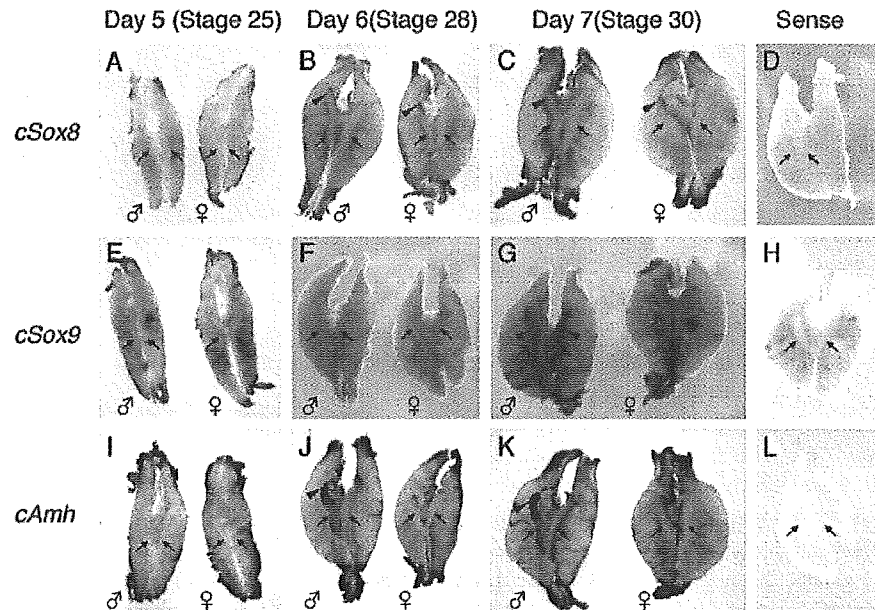
## Materials and methods

**Chicken embryos.** Fertilized chicken eggs were obtained from local suppliers (Ingham, Brisbane, Australia and Saitama Experimental Animal Supply, Saitama, Japan) and maintained at 18 °C until use. Eggs were transferred to an incubator at 37.5 °C and allowed to develop for 5, 6 or 7 days. Staging was confirmed at dissection according to Hamburger and Hamilton [39]. The entire urogenital ridge of each embryo was explanted for whole-mount *in situ* hybridization. Sexing was performed by PCR as described elsewhere [40] using genomic DNA purified from a hind limb of each embryo.

**Amplification of HMG box sequences.** Total RNA was isolated from left and right gonads of day 6 male embryos by standard methods [41]. RNA (0.5 µg) was then treated with DNaseI and first-strand cDNA was synthesized using M-MLV reverse transcriptase (Invitrogen) according to the manufacturer's protocol. For amplification of the HMG box, the PCR reaction was carried out in a solution containing 1 x NH<sub>4</sub> buffer (Bioline), 100 M MgCl<sub>2</sub>, 100 µM dNTPs, 0.4 µM primers and 0.5 unit Biotaq DNA polymerase (Bioline) with 4.5 min denaturation at 95 °C followed by 40 cycles of amplification at 95 °C for 30 s and 57 °C for 30 s. The PCR product was cloned into pGEM-T Easy (Promega). Sequencing was performed using the BigDye Terminator v3.1 Cycle Sequencing Kit (Applied Biosystems) and M13 reverse primer, and electrophoresis was carried out by the Australian Genome Research Facility, Brisbane, Australia. Primer sequences used were as follows; G7A1: 5'-AGC G(A/G)C CCA TGA ACG C(A/C/G/T)T T-3' and G7B1: 5'-CGC (C/T)GG TA(C/T) TT(A/G) TA(A/G) TC(A/C) GGG T-3'. The PCR reaction was also carried out using genomic DNA as a template.

**RT-PCR of *Sox* genes, *Amh* and *Actin*.** The left and right gonads of staged, sexed embryos were pooled (ten and five embryos of each sex for day 6 and day 7, respectively) to isolate total RNA using the RNeasy Mini kit (Qiagen) with the optional on-column DNase digestion with the RNase-free DNase set. The first-strand cDNA was synthesized from 1 µg of total RNA using Power-

Figure 1. Whole-mount *in situ* hybridization of *cSox8*, *cSox9* and *cAmh* in the chicken embryonic gonad/mesonephros. In each panel, male ( $\delta$ ) and female ( $\eta$ ) gonad/mesonephros are left and right, respectively. Probes used are shown at the left of each panel. The samples in A–C, E–G and I–K were hybridized with antisense probe. In D and L a day 6 sample hybridized with sense probe. In H a day 7 sample was hybridized with sense probe. Developmental stages (days and Hamburger-Hamilton stage) of gonad/mesonephros are labeled above. Arrow shows the position of gonad. Arrowheads point to regions of positive staining.



Script reverse transcriptase (Clontech) and oligodT. PCR amplification was carried out using the QuantiTect SYBR Green PCR kit (Qiagen) with uracil-N-glycosylase and the 7900HT Sequence Detection System (Applied Biosystems). Samples were incubated at 50°C for 2 min, then 95°C for 15 min, followed by 40 cycles of amplification at 94°C for 30 s, 54.2°C for 1 min and 72°C for 1 min. For the amplification of *cSox8* and *cSox9*, 85.4°C for 15 sec was added after each 72°C step of each amplification cycle. Primer sequences used were as follows; *cSox3*-1: 5'-GCACCAGCACTACCAGAG-3' and *cSox3*-2: 5'-CGA ATG CGG ACA CGA ACC) for *cSox3* [29], *cSox4*F: 5'-TCG GGG GAT TGG CTG GAG TC-3' and *cSox4*R: 5'-CTC AGC CGA TCC TCG TTT CC-3' for *cSox4*, *cSox8*RTF: 5'-CTA CAA GGC TGA CAG CGG GC-3' and *cSox8*RTR: 5'-AGG CCG GGC TCT TGT GAG TC-3' for *cSox8*, *cSox9*F: 5'-CCC CAA CGC CAT CTT CAA-3' and *cSox9*R: 5'-CTG CTG ATG CCG TAG GTA-3' for *cSox9*, *cSox11*F2: 5'-AAG CAG GAG GCG GAC GAC GA-3' and *cSox11*R2: 5'-CGC CCC GCA CCT CCT CGT AG-3' for *cSox11*, *cAmh*-1: 5'-GTG GAT GTG GCT CCC TAC CC-3' and *cAmh*-2: 5'-GCA GCA CCG AGG GCT CCT CC-3' for *cAmh* [29] and *Actin*-1: 5'-TGG ATG ATG ATA TTG CTG C-3' and *Actin*-2: 5'-ATC TTC TCC ATA TCA TCC C-3' [29] for *Actin*. To calculate the relative amount of gene expression levels, the  $\Delta\Delta C_T$  method was used. Three independent pooled samples were analyzed. Maximum average values were set as 100%.

For the RT-PCR amplification of *cSox12* and *cSox14*, the same cDNA for the real-time RT-PCR was used. The PCR reaction was carried out in the same solution as HMG box amplification with 4.5 min denaturation at 95°C followed by 40 cycles of amplification at 95°C for

30 s and 50°C for 30 s. Primer sequences used were as follows; *cSox12*F: 5'-AGA TCT CCA AGC GCC TGG GTC G-3' and *cSox12*R: 5'-GGT AGT CGG CCA TGT GCT TG-3' for *cSox12*, *cSox14*F: 5'-GAG GTT CCT CAC ACC TTG GC-3' and *cSox14*R: 5'-ACA CGG AGG AAT CCC AGT CC-3' for *cSox14*.

**Probes.** The previously reported *cAmh* probe [9] was obtained by RT-PCR amplification of an 821-bp fragment, using primers *cAMHRTF* (5'-ACG GTG CGC GCC CAC TGG CAG G-3') and *cAMHRTR* (5'-ACG TCG TGA CCT GCA AGC CCT C-3') and RNA prepared from 5.5-day-old whole embryo. The *cSox8* probe was cloned by PCR using primers *chSox8C2F* (5'-CTG CAG AGC TCC AAC TAC TAC A-3') and *chSox8C2R* (5'-GAG CTC TGT CCT TTT GGA GAG T-3') and chicken genomic DNA as the template. The fragment corresponds to nucleotides 1228–1589 of the *cSox8* mRNA sequence (accession No. AF228664). PCR products of *cAmh* and *cSox8* were cloned into the pGEM-T Easy vector. The *cSox9* probe was reported previously by Kent et al. [11]. The *cSox11* fragment was cloned by *Sac*I digestion of *cSox11* cDNA and subsequent insertion into pBluescriptII KS vector. The fragment corresponds to nucleotides 667–967 of the *cSox11* mRNA sequence (accession No. AB012237). The *cSox4* probe was obtained by *Ksp*I digestion of *cSox4* cDNA and subsequent insertion into pBluescriptII KS vector. The fragment corresponds to nucleotides 576–965 of the chicken *Sox4* mRNA sequence (accession No. AY493693).

**In situ hybridization.** Sense and antisense digoxigenin-labeled RNA probes were generated by *in vitro* transcrip-

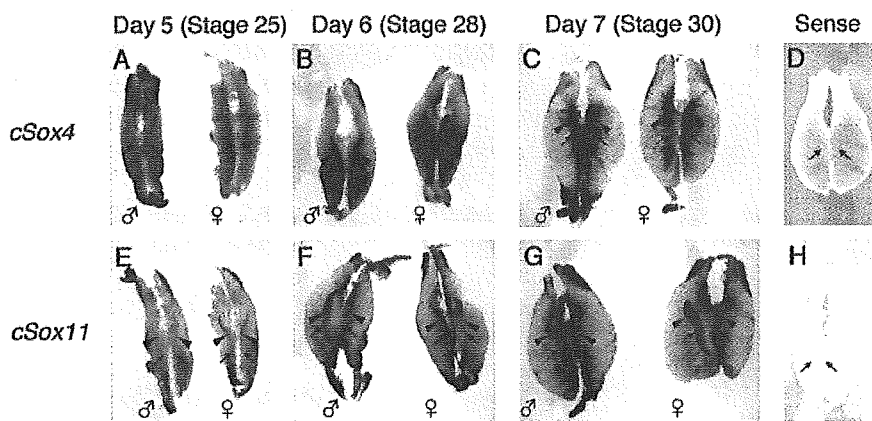


Figure 2. Whole-mount *in situ* hybridization of *cSox4* and *cSox11* in the chicken embryonic gonad/mesonephros. In each panel, male ( $\delta$ ) and female ( $\eta$ ) gonad/mesonephros are left and right, respectively. Probes used are shown at the left of each panel. A–C and E–G were hybridized with anti-sense probe. D and H show day 6 samples hybridized with sense probe. Developmental stages (days and Hamburger-Hamilton stage) of gonad/mesonephros are labeled above. Arrow shows the position of gonad. Arrowheads point to regions of staining.

tion. Whole mount *in situ* hybridization was performed as described using the maleic acid buffer (MABT) method [42]. Experiments were carried out at least twice for each probe, with similar results.

### Results and discussion

To compare the temporospatial expression of *cSox8* and *cAmh* in embryonic gonads, we employed whole-mount *in situ* hybridization analysis using female and male gonad/mesonephros complexes isolated from day 5, 6 and 7 chicken embryos (Hamburger and Hamilton stages 25, 28 and 30, respectively [39]). These stages cover the temporal window at which sexual dimorphism in the gonad first becomes apparent [43]. In addition to providing spatial information relating to gene expression, whole-mount *in situ* hybridization is commonly used as a semiquantitative guide to gene expression levels between different tissues hybridized with the same probe and incubated under the same conditions, as in the experiments described below.

As expected, *cAmh* was expressed at higher levels in male than in female gonads at day 6 and 7 (fig. 1J, K). Expression levels in the right male gonads were higher than in the left, possibly reflecting the asymmetric development of avian genital ridges [43]. We did not observe expression of *cAmh* at day 5 (fig. 1I), even though Oréal et al. [28] reported that *cAmh* is expressed weakly and at similar levels in male and female gonads at day 5 by section *in situ* hybridization. This may reflect lower sensitivity of our whole mount *in situ* hybridization method.

Previous workers have reported that male-specific high-level expression of *cSox9* is preceded by expression of *cAmh* in the chick [28, 29]. We analyzed the temporal expression of *cSox9* in chicken embryos. No signal was observed in male or female gonads at day 5 or day 6 (fig. 1E, F). High levels of *cSox9* expression were observed in day 7 male gonads, while no signal was observed in

the day 7 female (fig. 1G). This compares to the results of Oréal et al. [28] who described very faint expression of *cSox9* in day 6 gonads by *in situ* hybridization using sections. Our data demonstrate high levels of *cAmh* expression in day 6 male gonad, preceding the high levels of *cSox9* expression first detected in day 7 male gonad. They suggest that SOX9 is not responsible for the male-specific up-regulation of *cAmh*, but may play a role in the maintenance and/or amplification of *cAmh* expression in the male gonads once transcription is initiated. Our results support the previous observation that the male-specific high levels of *cAmh* expression precede testicular *cSox9* expression [28, 29].

We next examined expression of *Sox8*. At day 5, no *cSox8* expression was observed (fig. 1A). At day 6 and 7, *cSox8* expression was observed at the anterior tip of both male and female right gonads at similar levels (fig. 1B, C). This expression profile is different from that of *cAmh*, both in spatial distribution of transcripts and degree of sex specificity, suggesting that SOX8 could not be responsible for sex-specific up-regulation of *cAmh* in chicken.

The expression patterns of mouse and chicken *Sox8* imply that the functions of SOX8 are conserved in most but not all tissues between the two species. For example, *Sox8* is expressed in brain, skeletal muscle, eye, somite, dermomyotome, limb, digits, gut, spinal cord and dorsal root ganglia in both species [30, 31, 44]. However, some differences are evident in embryonic heart and gonad: in chicken, *cSox8* is expressed in the embryonic heart, testis and ovary, whereas in mouse, *Sox8* expression occurs predominantly in the embryonic testis, but not in the ovary or heart [31, 44]. Given these observations, SOX8 may contribute to the male-specific activation of *Amh* expression during gonadogenesis in mice but not chicken.

In mouse, only two SOX proteins, SOX8 and SOX9, have been identified as regulators of *Amh* expression in the embryonic gonad [26]. Based on our data, and previous studies [28, 29], neither SOX8 nor SOX9 can be responsible for the onset of high levels of *cAmh* expression



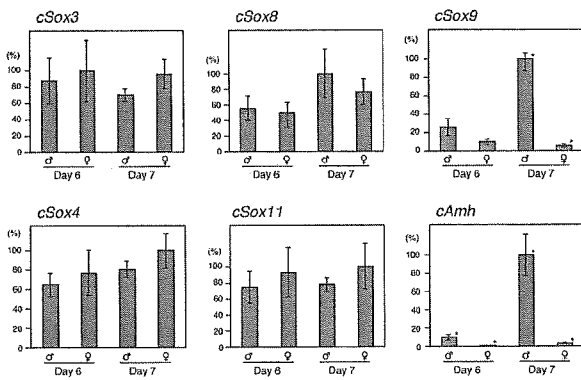


Figure 3. Quantitative, real-time RT-PCR analysis of *Sox* and *Amh* gene expression. Averages of three independent trials are shown as bars, with SEs shown as lines. Values marked with \* were significantly different between males ( $\delta$ ) and females ( $\text{♀}$ ) ( $p = 0.0017$ ,  $0.0047$  and  $0.012$  for *cSox9* at day 7, *cAmh* at day 6 and 7, respectively, using a two-sample equal variance t-test). Others were not significantly different between males and females ( $p = 0.81$ ,  $0.24$ ,  $0.74$ ,  $0.52$ ,  $0.17$ ,  $0.67$ ,  $0.38$ ,  $0.64$ ,  $0.49$  for *cSox3* at day 6 and 7, *cSox8* at day 6 and 7, *cSox9* at day 6, *cSox4* at day 6 and 7, and *cSox11* at day 6 and 7, respectively).

in chicken, even though two SOX-binding sites are predicted in the *cAmh* promoter region. These observations prompted us to search for other *Sox* genes expressed in chicken male gonads that could be considered as candidate regulators of *Amh* expression. We conducted the analysis at day 6, since at this stage *cAmh* is expressed at high levels in male gonads while *cSox9* is either not expressed or expressed at a very low level.

We utilized degenerate RT-PCR on purified day 6 male gonad RNA using generic *Sry*-type HMG box primers to generate fragments for cloning into a plasmid vector. Twenty independent clones were sequenced, revealing that 12 clones were *cSox4* [45], 7 were *cSox11* [46] and 1 was *cSox9* [47].

One possible explanation for these results is that the degenerate primers used show a bias for amplification of *cSox4* and *cSox11* templates. To examine this possibility, we used the same degenerate primers to amplify *Sox* fragments from genomic DNA, in which all intronless *Sox* genes (*Sox1*, -2, -3, -4, -11, -12, -14, -21) capable of amplification by the primers are represented in equal proportions. Among ten clones amplified, none was *cSox4* or *cSox11*. Thus, primer bias does not explain our data relating to *cSox4* and *cSox11* expression in developing chicken gonads.

*cSox4* and *cSox11* are expressed in male gonads at day 6, prompting us to examine the expression profiles of each in male and female gonads through the sex determination window. If both or either is expressed preferentially in male gonads, they could be considered a candidate for regulation of the *cAmh* gene. To evaluate the expression patterns of *cSox4* and *cSox11* in embryonic gonads, we

employed whole-mount *in situ* hybridization analysis at the same stages previously used to profile *cSox8*, *cSox9* and *cAmh* expression. *cSox4* and *cSox11* signals were detected at similar levels in male and female gonads at all stages examined (fig. 2) suggesting that neither of them plays a role in sex-specific regulation of *Amh*.

The identification of *Sox* genes that are expressed in chicken embryonic gonads at day 5, 6 and 7 was previously attempted by McBride et al. [6]. Using RT-PCR amplification of the conserved *Sry*-type HMG box domain from RNA samples prepared from testes with mesonephroi attached, they found expression of *cSox3*, *cSox4*, *cSox9*, *cSox11*, *cSox12* and *cSox14*. Our data confirm that *cSox4*, *cSox9* and *cSox11* are indeed expressed, as is *cSox3* (see below); however, we amplified the HMG box from day 6 gonad only, and this difference along with the differences in PCR primers, may explain the discrepancies in the data for *cSox12* and *cSox14*. Moreover, day 6 male gonad expresses *cSox4* and *cSox11* transcripts so abundantly that RT-PCR cloning is difficult for *Sox* genes expressed at low levels.

To examine the levels of gene expression quantitatively, we utilized RT-PCR and real-time RT-PCR analyses using RNAs isolated from pooled, sexed embryonic gonads at days 6 and 7 (fig. 3). As expected, *cAmh* and *cSox9* were expressed at different levels between males and females at day 7. At day 6, the expression levels of *cAmh* were statistically different between males and females ( $p < 0.005$ ) while the expression levels of *cSox9* were not ( $p > 0.1$ ). However, *cSox3*, *cSox4*, *cSox8* and *cSox11* were expressed at similar levels between males and females at days 6 and 7, suggesting that none of these *Sox* genes is responsible for the male-specific up-regulation of *cAmh* expression.

We were unable to amplify *cSox12* and *cSox14* sequences by RT-PCR from chicken embryonic gonads. As a positive control, chicken genomic DNA was included as template. Signals were observed at expected size of 108 bp for *cSox12* and 331 bp for *cSox14* only from genome template, but not from gonad RNA samples, showing that neither gene is expressed in embryonic gonads at day 6 and day 7 (data not shown).

Previous studies have eliminated *cSox3* as a candidate for male-specific up-regulation of *Amh* expression because *cSox3* is expressed at similar levels in the male and female gonads at the sex-determining window [28, 29]. Our present data support this conclusion. We rule out *cSox8* because it is expressed in a different spatial pattern to *Amh*, and *cSox12* and -14 because they are not expressed in gonads at sex-determining stages at all. We exclude *cSox4* and *cSox11* also, on the basis of equivalent expression levels between male and female. It is formally possible that *cSox4* and *cSox11* might be expressed in Sertoli cells in the male (the site of *Amh* expression) and in another cell lineage in females, in which *Amh* is

not expressed, but we consider this unlikely, especially considering that all genes found to be involved in sex-specific development of the gonads to date show a sexually dimorphic pattern of gene expression in fetal gonads when examined by whole-mount *in situ* hybridization. However, one still cannot exclude the possibility of SOX protein-mediated regulation of *cAmh* gene expression, and further extensive cloning of *cSox* genes may be necessary to discover a *Sox* gene expressed predominantly in chicken embryonic testis.

Alternatively, we have to consider that sex-specific *Amh* up-regulation is not mediated by SOX proteins in birds. Even though the putative SF1-binding site, like the two SOX-binding site in the *Amh* promoter, is conserved between mouse and chicken [28], and *cSfl* is co-expressed with *cAmh* at day 7 of chicken embryonic testis [15], the expression profiles of mouse and chicken *Sfl* show major differences. Before testis cord formation, *Sfl* is expressed at similar levels in males and females in both species, while subsequently, chicken *Sfl* expression is maintained in the testis, but is up-regulated in the ovary [12, 15, 29]. The opposite expression pattern is reported for mouse *Sfl* [reviewed in ref. 48]. This difference could be explained by the possibility that *Sfl* functions in more steroidogenically active tissue (testis in mammals and ovary in birds), or that *Sfl* may not be associated with testis formation in birds [12]. Either way, the expression profile of *cSfl*, like that of *cSox9* [28] and *cSox8* (this study), suggests that it is not responsible for male-specific up-regulation of *cAmh* expression during chicken gonadogenesis. Since both SF1 and SOX proteins are required for normal levels of *Amh* expression during sex determination in mouse [27], this may imply that there is a different mechanism of *cAmh* regulation in chicken compared with mouse, and that SOX protein is not a causative factor for sex-specific expression of *cAmh*.

Gonadal expression of *Sox8*, which has an evolutionarily conserved coding protein among vertebrates, has been studied in mouse, chicken and red-eared slider turtle [31, 49]. *Sox8* is expressed in the developing testes of all three species, implying a functional significance, but in chicken and turtle, *Sox8* is also expressed in the ovary. So far, up-regulation of mouse *Amh* is the only known molecular function for the SOX8 protein [26]. If this function is conserved among vertebrates, chicken SOX8 may have a protein partner which is expressed in males to activate or in females to suppress *cAmh*. Some genes are expressed sex specifically during gonadal differentiation in the mouse, including *Sfl* [13], *Wtl* [50], *Gata4* [14], *Lhx9* [51], *Wnt-4* [52] and *Dax1* [53]. However, chicken homologues of these genes are not candidates because they are expressed in both developing testis and ovary while *cAmh* is differentially expressed [15, 29]. *Dmrt1* is expressed only in developing testis in mouse, while

chicken *Dmrt1* is expressed in both developing gonads with higher levels in testis, suggesting that it is not such a factor [15, 54]. The identification of a chicken SOX8-binding partner may clarify this possibility. Finally, further analysis of the *cAmh* promoter may reveal whether SOX proteins play a role in its up-regulation, and whether similarities exist in the mechanisms that regulate *Amh* expression in birds and mammals.

**Acknowledgements.** We thank M. Hargrave, K. Löffler and J. Bowles and members of the Koopman laboratory for technical advice and constructive criticism, and D. Wilhelm and F. Martinson for critical reading of this manuscript. P. K. is a Professorial Research Fellow of the Australian Research Council.

- Gubbay J., Collignon J., Koopman P., Capel B., Economou A., Münsterberg A. et al. (1990) A gene mapping to the sex-determining region of the mouse Y chromosome is a member of a novel family of embryonically expressed genes. *Nature* **346**: 245–250
- Sinclair A. H., Berta P., Palmer M. S., Hawkins J. R., Griffiths B. L., Smith M. J. et al. (1990) A gene from the human sex-determining region encodes a protein with homology to a conserved DNA-binding motif. *Nature* **346**: 240–244
- Koopman P., Gubbay J., Vivian N., Goodfellow P. and Lovell-Badge R. (1991) Male development of chromosomally female mice transgenic for Sry. *Nature* **351**: 117–121
- Coriat A.-M., Muller U., Harry J. L., Uwanogho D. and Sharpe P. T. (1993) PCR amplification of SRY-related gene sequences reveals evolutionary conservation of SRY-box Motif. *PCR Methods Appl.* **2**: 218–222
- Griffiths R. (1991) The isolation of conserved DNA sequences related to the human sex determining region Y gene from the lesser black-backed gull (*Larus fuscus*). *Proc. R. Soc. Lond. B.* **224**: 123–128
- McBride D., Sang H. and Clinton M. (1997) Expression of Sry-related genes in the developing genital ridge/mesonephros of the chick embryo. *J. Reprod. Fertil.* **109**: 59–63
- Tiersch T. R., Mitchell M. J. and Wachtel S. S. (1991) Studies on the phylogenetic conservation of the SRY gene. *Hum. Genet.* **87**: 571–573
- Clinton M. (1998) Sex determination and gonadal development: a bird's eye view. *J. Exp. Zool.* **281**: 457–465
- Carré-Eusèbe D., Clemente N. di, Rey R., Pieau C., Vigier B., Josso N. et al. (1996) Cloning and expression of the chick anti-Müllerian hormone gene. *J. Biol. Chem.* **271**: 4798–4804
- Morais da Silva S., Hacker A., Harley V., Goodfellow P., Swain A. and Lovell-Badge R. (1996) Sox9 expression during gonadal development implies a conserved role for the gene in testis differentiation in mammals and birds. *Nat. Genet.* **14**: 62–68
- Kent J., Wheatley S. C., Andrews J. E., Sinclair A. H. and Koopman P. (1996) A male-specific role for SOX9 in vertebrate sex determination. *Development* **122**: 2813–2822
- Smith C. A., Smith M. J. and Sinclair A. H. (1999b) Expression of chicken steroidogenic factor-1 during gonadal sex differentiation. *Gen. Comp. Endocrinol.* **113**: 187–196
- Ikeda Y., Shen W. H., Ingraham H. A. and Parker K. L. (1994) Developmental expression of mouse steroidogenic factor-1, an essential regulator of the steroid hydroxylases. *Mol. Endocrinol.* **8**: 654–662
- Viger R. S., Mertineit C., Trasler J. M. and Nemer M. (1998) Transcription factor GATA-4 is expressed in a sexually dimorphic pattern during mouse gonadal development and is a potent activator of the Müllerian inhibiting substance promoter. *Development* **125**: 2665–2675
- Oréal E., Mazaud S., Picard J.-Y., Magre S. and Carré-Eusèbe D. (2002) Different patterns of anti-Müllerian hormone expres-

- sion, as related to DMRT1, SF-1, WT1, GATA-4, Wnt-4, and Lhx9 expression, in the chick differentiating gonads. *Dev. Dyn.* **225**: 221–232
- 16 Wegner M. (1999) From head to toes: the multiple facets of Sox proteins. *Nucleic Acids Res.* **15**: 1409–1420
  - 17 Bowles J., Schepers G. and Koopman P. (2000) Phylogeny of the SOX family of developmental transcription factors based on sequence and structural indicators. *Dev. Biol.* **227**: 239–255
  - 18 Schepers G. E., Teasdale R. D. and Koopman P. (2002) Twenty pairs of Sox: extent, homology, and nomenclature of the mouse and human sox transcription factor gene families. *Dev. Cell.* **3**: 167–170
  - 19 Foster J. W., Dominguez-Steglich M. A., Guioli S., Kowk C., Weller P. A., Weissenbach J. et al. (1994) Campomelic dysplasia and autosomal sex reversal caused by mutations in an SRY-related gene. *Nature* **372**: 525–30
  - 20 Wagner T., Wirth J., Meyer J., Zabel B., Held M., Zimmer J. et al. (1994) Autosomal sex reversal and campomelic dysplasia are caused by mutations in and around the SRY-related gene SOX9. *Cell* **79**: 1111–120
  - 21 Vidal V. P. I., Chaboissier M.-C., Rooij D. G. de and Schedl A. (2001) Sox9 induces testis development in XX transgenic mice. *Nat. Genet.* **28**: 216–17
  - 22 Josso N., Clemente N. di and Gouédard L. (2001) Anti-Müllerian hormone and its receptors. *Mol. Cell. Endocrinol.* **179**: 25–32
  - 23 Nachtigal M. W., Hirokawa Y., Enyeart-VanHouten D. L., Flanagan J. N., Hammer G. D. and Ingraham H. A. (1998) Wilms' tumor 1 and Dax-1 modulate the orphan nuclear receptor SF-1 in sex-specific gene expression. *Cell* **93**: 445–454
  - 24 Tremblay J. J. and Viger R. S. (1999) Transcription factor GATA-4 enhances Müllerian inhibiting substance gene transcription through a direct interaction with the nuclear receptor SF-1. *Mol. Endocrinol.* **13**: 1388–1401
  - 25 Santa Barbara P. de, Bonneaud N., Boizet B., Desclozeaux M., Moniot B., Südbeck P. et al. (1998) Direct interaction of SRY-related protein SOX9 and steroidogenic factor 1 regulates transcription of the human anti-Müllerian hormone gene. *Mol. Cell. Biol.* **18**: 6653–6665
  - 26 Schepers G., Wilson M., Wilhelm D. and Koopman P. (2003) SOX8 is expressed during testis differentiation in mice and synergizes with SF1 to activate the Amh promoter in vitro. *J. Biol. Chem.* **278**: 28101–28108
  - 27 Arango N. A., Lovell-Badge R. and Behringer R. R. (1999) Targeted mutagenesis of the endogenous mouse Mis gene promoter: in vivo definition of genetic pathways of vertebrate sexual development. *Cell* **99**: 409–419
  - 28 Oréal E., Picau C., Mattei M. G., Josso N., Picard J.-Y., Carré-Eusèbe D. et al. (1998) Early expression of AMH in chicken embryonic gonads precedes testicular SOX9 expression. *Dev. Dyn.* **212**: 522–532
  - 29 Smith C. A., Smith M. J. and Sinclair A. H. (1999a) Gene expression during gonadogenesis in the chicken embryo. *Gene* **234**: 395–402
  - 30 Takada S. and Koopman P. (2003) Origin and possible roles of the Sox8 transcription factor gene during sexual development. *Cytogenet. Genome Res.* **101**: 212–218
  - 31 Schepers G. E., Bullejos M., Hosking B. M. and Koopman P. (2000) Cloning and characterisation of the Sry-related transcription factor gene Sox8. *Nucleic Acids Res.* **28**: 1473–1480
  - 32 Wright E., Hargrave M. R., Christiansen J., Cooper L., Kun J., Evans T. et al. (1995) The Sry-related gene Sox-9 is expressed during chondrogenesis in mouse embryos. *Nat. Genet.* **9**: 15–20
  - 33 Pusch C., Hustert E., Pfeifer D., Südbeck P., Kist R., Roe B. et al. (1998) The SOX10/Sox10 gene from human and mouse: sequence, expression, and transactivation by the encoded HMG domain transcription factor. *Hum. Genet.* **103**: 115–123
  - 34 Collignon J., Sockanathan S., Hacker A., Cohen-Tannoudji M., Norris D., Rastan S. et al. (1996) A comparison of the properties of Sox-3 with Sry and two related genes, Sox-1 and Sox-2. *Development* **122**: 509–520
  - 35 Smits P., Li P., Mandel J., Zhang Z., Deng J. M., Behringer R. R. et al. (2001) The transcription factors L-Sox5 and Sox6 are essential for cartilage formation. *Dev. Cell* **1**: 277–290
  - 36 Downes M. and Koopman P. (2001) SOX18 and the transcriptional regulation of blood vessel development. *Trends Cardiovasc. Med.* **11**: 318–324
  - 37 Kanai-Azuma M., Kanai Y., Gad J. M., Tajima Y., Taya C., Kurohmaru M. et al. (2002) Depletion of definitive gut endoderm in Sox17-null mutant mice. *Development* **129**: 2367–2379
  - 38 Pennisi D., Bowles J., Nagy A., Muscat G. and Koopman P. (2000) Mice null for Sox18 are viable and display a mild coat defect. *Mol. Cell. Biol.* **20**: 9331–9336
  - 39 Hamburger V. and Hamilton H. L. (1951) A series of normal stages in the development of the chick embryo. *J. Morphol.* **88**: 49–92
  - 40 Clinton M., Haines L., Belloir B. and McBride D. (2001) Sexing chick embryos: a rapid and simple protocol. *Br. Poult. Sci.* **42**: 134–138
  - 41 Chomczynski P. and Sacchi N. (1987) Single-step method of RNA isolation by acid guanidinium thiocyanate-phenol-chloroform extraction. *Anal. Biochem.* **162**: 156–159
  - 42 Xu Q. and Wilkinson D. (1998) In situ hybridization of mRNA with hapten labelled probes. In: *In Situ Hybridization: A Practical Approach*, 2nd ed., pp. 87–106, Wilkinson D. (ed.), Oxford University Press, Oxford
  - 43 Romanoff A. L. (1960) *The Avian Embryo: Structural and Functional Development*, Macmillan, New York
  - 44 Bell K. M., Western P. S. and Sinclair A. H. (2000) SOX8 expression during chick embryogenesis. *Mech. Dev.* **94**: 257–260
  - 45 Maschhoff K. L., Anziano P. Q., Ward P. and Baldwin H. S. (2003) Conservation of Sox4 gene structure and expression during chicken embryogenesis. *Gene* **320**: 23–30
  - 46 Uwanogho D., Rex M., Cartwright E. J., Pearl G., Healy C., Scotting P. J. et al. (1995) Embryonic expression of the chicken Sox2, Sox3 and Sox11 genes suggests an interactive role in neuronal development. *Mech. Dev.* **49**: 23–36
  - 47 Healy C, Uwanogho D. and Sharpe P. T. (1999) Regulation and role of Sox9 in cartilage formation. *Dev. Dyn.* **215**: 69–78
  - 48 Parker K. L. and Schimmer B. P. (1997) Steroidogenic factor 1: a key determinant of endocrine development and function. *Endocr. Rev.* **18**: 361–377
  - 49 Takada S., DiNapoli L., Capel B. and Koopman P. (2004) Sox8 is expressed at similar levels in gonads of both sexes during the sex determining period in turtles. *Dev. Dyn.* **231**: 387–395
  - 50 Pelletier J., Schalling M., Buckler A. J., Rogers A., Haber D. A. and Housman D. (1991) Expression of the Wilms' tumor gene WT1 in the murine urogenital system. *Genes. Dev.* **5**: 1345–1356
  - 51 Birk O. S., Casiano D. E., Wassif C. A., Cogliati T., Zhao L., Zhao Y. et al. (2000) The LIM homeobox gene Lhx9 is essential for mouse gonad formation. *Nature* **403**: 909–913
  - 52 Vainio S., Heikkilä M., Kispert A., Chin N. and McMahon A. P. (1999) Female development in mammals is regulated by Wnt-4 signalling. *Nature* **397**: 405–409
  - 53 Swain A., Zanaria E., Hacker A., Lovell-Badge R. and Camerino G. (1996) Mouse Dax1 expression is consistent with a role in sex determination as well as in adrenal and hypothalamus function. *Nat. Genet.* **12**: 404–409
  - 54 Raymond C. S., Kettlewell J. R., Hirsch B., Bardwell V. J. and Zarkower D. (1999) Expression of Dmrt1 in the genital ridge of mouse and chicken embryos suggests a role in vertebrate sexual development. *Dev. Biol.* **215**: 208–220

## Gene expression profiling of human atrial myocardium with atrial fibrillation by DNA microarray analysis

Ruri Ohki<sup>a</sup>, Keiji Yamamoto<sup>a,\*</sup>, Shuichi Ueno<sup>a</sup>, Hiroyuki Mano<sup>b</sup>, Yoshio Misawa<sup>c</sup>  
Katsuo Fuse<sup>c</sup>, Uichi Ikeda<sup>a</sup>, Kazuyuki Shimada<sup>a</sup>

<sup>a</sup>Division of Cardiovascular Medicine, Jichi Medical School, Minamikawachi-Machi, Tochigi 329-0498, Japan

<sup>b</sup>Division of Functional Genomics, Jichi Medical School, Minamikawachi-Machi, Tochigi 329-0498, Japan

<sup>c</sup>Division of Cardiovascular Surgery, Jichi Medical School, Minamikawachi-Machi, Tochigi 329-0498, Japan

Received 16 December 2003; received in revised form 31 March 2004; accepted 5 May 2004

Available online 9 August 2004

### Abstract

**Background:** Atrial fibrillation (AF) is the most frequently encountered arrhythmia in the clinical setting. However, a comprehensive investigation of the molecular mechanism of AF has not been performed. The aim of this study was to clarify transcriptional profiling of genes modulated in the atrium of AF patients using DNA microarray technology.

**Methods:** We obtained 17 fresh cardiac specimens, right atrial appendages, isolated from 10 patients with normal sinus rhythm and seven chronic AF patients who underwent cardiac surgery. Affymetrix GeneChip (Human Genome U95A) investigating 12,000 human genes was used for each specimen. Quantitative analysis of selected genes was performed by the real-time PCR method.

**Results:** The left atrial diameter in the AF group was greater than that in the sinus rhythm group. We could identify 33 AF-specific genes that were significantly activated (>1.5-fold), compared with the sinus rhythm group, including an ion channel, an antioxidant, an inflammation, three cell growth/cell cycle, three transcription such as nuclear factor-interleukin 6-beta, several cell signaling and several protein genes, and seven expressed sequence tags (ESTs). In contrast, we found 63 sinus rhythm-specific genes, including several cell signaling/communication such as sarcoplasmic reticulum Ca<sup>2+</sup>-ATPase 2, several cellular respiration and energy production and two antiproliferative or negative regulator of cell growth genes, and 22 ESTs.

**Conclusions:** The present study demonstrated that about one hundred genes were modulated in the atria of AF patients. These findings suggest that these genes may play critical roles in the initiation or perpetuation of AF and the pathophysiology of atrial remodeling.

© 2004 Elsevier Ireland Ltd. All rights reserved.

**Keywords:** Atrial fibrillation; Genes; Microarray; Myocardium

### 1. Introduction

Atrial fibrillation (AF) is the most common sustained cardiac arrhythmia and the major cardiac cause of stroke [1]. The Framingham Study [2] reported a sixfold increase in the incidence of stroke in patients with AF, compared with age-, sex-, and blood pressure-adjusted control subjects. In addition, the rapid heart rate resulting from AF can bring about a number of adverse outcomes including congestive heart failure and tachycardia-related

cardiomyopathy [3,4]. The molecular research of AF has been focused mainly at various ion channels and at proteins involved in calcium homeostasis, because AF modifies the electrical properties of the atrium in a manner that promotes its occurrence and maintenance. This arrhythmogenic electrophysiological remodeling is well established. However, a comprehensive investigation of the molecular mechanism causing AF has not been performed.

With the recent discovery of the complete sequence of the human genome, as well as the genomes of other organisms, new high-throughput approaches to studying these complex pathways have been made possible. By

\* Corresponding author. Tel.: +81 285 58 7344; fax: +81 285 44 5317.

E-mail address: kyamamoto@jichi.ac.jp (K. Yamamoto).